Nicolas Randazzo
1056910
Email: randazn@mcmaster.ca
Phone: 905-578-5035

Thesis
Carbon and Oxygen Isotope Effects in Synthesized Carbonates at 25 ^{o}C
By Nicolas Randazzo

A Thesis
Submitted to the School of Geography and Earth Sciences
In Partial Fulfilment of the Requirements
for the Degree
Master of Science
McMaster University

Descriptive Note

MASTER OF SCIENCE (2016) McMaster University

School of Geography and Earth Sciences Hamilton, Ontario

TITLE: Carbon and Oxygen Isotope Effects in Synthesized Calcite at 25 ^{o}C
AUTHOR: Nicolas Randazzo

SUPERVISOR: Professor Sang-Tae Kim
NUMBER OF PAGES: VII, 84

Acknowledgments

First I would like to thank God, for nothing is possible without Him. I cannot stress enough the role that faith has had as a source of comfort and guidance during my academic career.

Special thanks go to Dr. Sang-Tae Kim for granting me the opportunity to complete this thesis research and for the numerous conversations we had discussing the data and how to best present it to the public. I also appreciate the effort and time he put towards helping advance my career as a scientist and for inviting me to co-author additional research with him. While my six year McMaster journey has come to a close, I cannot look forward without the knowledge that he helped me to achieve whatever lies ahead. You started out as my supervisor and are now a friend. Thanks also go to my committee members, Dr. Gregory Slater and Dr. Henry Schwarcz for their input into this manuscript

I am also grateful to Mohammed El-Shenawy for breathing new life into my project and for greatly assisting in my understanding of the stable isotope systematics of my system. These projects would not exist if it weren't for him. Though life has taken us in separate directions for the time being, I will never forget the conversations and time we spent together in the lab. God bless. I would also like to thank Martin Knyf for his valuable assistance and guidance throughout this project. He is a valuable asset to the lab and to the School of Geography and Earth Sciences. His patience, humour, selflessness, and hard-work did not go unnoticed and his love of science is truly an inspiration. I wish him all the best in his well-deserved retirement! I am also thankful to the Government of Ontario and McMaster University for funding me during the past two years and those who donated to the McMaster Research Group for Stable Isotopologues (MRSI), namely the American Chemical Society, the Petroleum Research Fund (ACS-PRF), Natural Science and Engineering Research Council (NSERC) Discovery Grant, Ontario Ministry of Research and Innovation, the Ontario Research Fund (MRI-ORF), and Canada Foundation for Innovation- Leaders Opportunity Fund (CFI-LOF) .

I also extend my gratitude to all of my family, especially my mother, father, and Dio, for their encouragement, support, motivation, patience, and willingness to do whatever they could to provide for me and help me succeed. I could not have done any of this without them all. I am who I am only because of them. Thanks also go out to my fellow MRSI lab mates Jillian Wyman, Chris Spencer, and Kesia Ie who have all completed their graduate career. The time we spent together both in the lab and out will always be remembered with fondness. I would also like to express my gratitude to all of my friends in the School of Geography and Earth Sciences. I am honoured to have had a role in your educational career and look forward to seeing how all of you will make the world a better place. Thank you also goes out to Dr. Maureen Padden, Salome Santos-Blaguski, Deane Maynard, Victoria Jarvis, Cassandra Lo, Alex Poulin and all other members of the SGES department who assisted me during the past two years. You are all remarkable people!

Finally, I thank everyone who played a role in my time at McMaster, both as a graduate and undergraduate student. My time here has truly expanded my mind and made an already curious boy more interested in the world around him. I also thank the numerous scientists and thinkers who have come before me, but still continue to inspire my academic life.

Abstract

Carbonate minerals have been abundant throughout Earth's geological history and the carbon and oxygen isotope ratios of carbonates can be used for paleoclimate reconstruction based upon the recognized stable isotopic relationship with the environmental factors. However, their accuracy is obscured by "non-equilibrium isotope effects" caused by physicochemical factors, such as solution chemistry, pH and precipitation rate. This study aimed to better understand these factors to improve the robustness of isotope-based paleotemperature proxy and assist in providing a reference frame for future research. Carbonates were synthesized using passive $CO_{2(g)}$ degassing at two different pH levels (~8.2 and ~11.07) through the dissolution of 5, 15 and 25 mmolal sodium bicarbonate ($NaHCO_3$) or sodium carbonate (NA_2CO_3) and calcium chloride dihydrate ($CaCl_2 \cdot 2H_2O$) at 25 ± 0.1 ºC. The $1000\ln^{18}\alpha_{(CaCO_3\text{-}H_2O)}$ and $1000\ln^{13}\alpha_{(CaCO_3\text{-}DIC)}$ values were then compared with established isotopic equilibrium values for oxygen and carbon. Samples were also synthesized in the presence of various concentrations of carbonic anhydrase (CA) and it was found that this enzyme may not influence kinetic isotope effects at higher precipitation rates. A positive, concentration based trend was found for the mid-pH solutions between $1000\ln^{13}\alpha_{(CaCO_3\text{-}DIC)}$ and $1000\ln^{18}\alpha_{(CaCO_3\text{-}H_2O)}$ values which began at the oxygen isotopic equilibrium value proposed by Kim and O'Neil (1997). This trend deviated upwards towards that of Coplen (2007) due to the kinetic influence of precipitation rate and degassing caused by the production of $CO_{2(aq)}$ as a by-product of the aforementioned reaction. The high pH solutions followed an opposite trend, with $1000\ln^{13}\alpha_{(CaCO_3\text{-}DIC)}$ continuing the enrichment trend but $1000\ln^{18}\alpha_{(CaCO_3\text{-}H_2O)}$ values declining and may have been caused by $CO_{2(aq)}$ not being produced in the high pH reactions. The DIC equilibration time at this pH took 7 days as shown by Kim et al. (2006) and not 45 days as discussed in Beck et al. (2005).

Table of Contents

List of Tables

List of Figures

Chapter 1:
Introduction and Background Information

Chapter 1

"If I have seen further than others,
it is by standing upon the shoulders of giants".
-Isaac Newton

1.1 Environmental Reconstruction of Paleoclimates using Stable Isotopes

In the last five decades, oxygen isotope fractionation factor between calcite and water has been used extensively to estimate paleotemperature in marine and continental carbonates which are precipitated under isotopic equilibrium (Epstein et al, 1953). Isotopic equilibrium describes the point where two substances (i.e. calcite and water) cease the exchange of stable isotopes. This can only be determined once chemical equilibrium has been established. However, the utilization of isotopes, such as those from oxygen, to determine paleotemperatures are obscured by factors such as kinetic effects from pH, growth rate and solution chemistry. Kim and O'Neil (1997) noted some non-equilibrium isotope effects which impacted the oxygen isotope fractionation factor of their system and theorized about a system responsible for the observed isotope effects, which Zeebe (1999) proposed to be caused by the effect of pH on the solution chemistry. The total amount of inorganic carbon species within a solution is known as the dissolved inorganic carbon (DIC) and is composed of CO_2* (i.e. the sum of aqueous carbon dioxide ($CO_{2(aq)}$) and carbonic acid (H_2CO_3) within the system), bicarbonate ion (HCO_3), and carbonate ion (CO_3^{2-}). The concentration and domination of these species is dependent on the pH of the solution. At low pH ($\leq$6) , CO_2^* is the most dominant, however, HCO_3 becomes the most abundant at mid-pH (6 to 9.5) and CO_3^{2-} is predominant at high pH ($\geq$ 9.5) (Beck et al., 2005; Kim et al., 2006).

The level of $CO_{2(aq)}$ within ocean water is related to the amount of $CO_{2(g)}$ within the atmosphere due to gas exchange caused by partial pressure gradients (Henry, 1803). For instance, if the pCO_2 over a body of water increases, due to factors such as anthropogenic $CO_{2(g)}$

emissions, the gas will diffuse into the water until equilibrium is established at the air-water interface. Upon the absorption of $CO_{2(g)}$ within the water, chemical reactions occur which reduce seawater pH and carbonate ion concentration as the $CO_{2(aq)}$ is converted into the other DIC species. These species interconvert to maintain chemical equilibrium. The conversion chemical equations are:

$$CO_{2(aq)} + H_2O \rightleftharpoons H_2CO_3$$
$$H_2CO_3 \rightleftharpoons HCO_3^- + H^+$$
$$HCO_3^- \rightleftharpoons CO_3^{2-} + H^+$$

The two apparent equilibrium constants exist because there are two dissociating reactions. These constants can be calculated using the following equations:

$$K_1 = ([HCO_3^-] + [H^+])/ H_2CO_3$$
$$K_2 = ([CO_3^{2-}] + [H^+])/ HCO_3^-$$

The constants established, constant values which are temperature, salinity, and pressure dependent (Drever, 1988). The constant value illustrates the relative amount of dissociation within the system. These equations can then be re-arranged so that the concentration of each individual DIC species can be calculated.

$$CO_2 = DIC/ (1+(K_1/ H^+) + K_1 K_2/ (H^+)^2)$$
$$HCO_3^- = DIC/ ((H^+/ K_1) + 1 + (K_2/ H^+))$$
$$CO_3^{2-} = DIC/ ((1 + (H^+)^2/ K_1 K_2) + (H^+/ K_2))$$

The pKa is calculated using the following equation:

$$pKa = -\log_{10}(K)$$

For example if K_1 is equal to $10^{-6.3}$ and K_2 is equal to $10^{-10.3}$, then pK_1 is 6.3 and pK_2 is 10.3. If the pH of the system is below 6.3, then $CO_{2(aq)}$ will be the dominant ion. If it is between 6.3 and 10.3, most of the DIC will be composed of HCO_3^-, and finally, if the pH is above 10.3, CO_3^{2-} will be present in the largest quantities.

The solubility of calcium carbonate is defined by its solubility product (K_{sp}), which describes how much dissolved ions can exist within a solution (i.e. water) before precipitation begins. The K_{sp} is calculated through the following equation:

$$K_{sp} = [Ca^{2+}][CO_3^{2-}]$$

The solubility product is constant for a given temperature and is unique to different minerals. The K_{sp} for $CaCO_3$ is a little uncertain, ranging from 3.7×10^{-9} to 8.7×10^{-9} at 25 °C, depending upon the literature source. If the molar concentration of Ca^{2+} and CO_3^{2-} exceed the K_{sp}, precipitation of $CaCO_3$ will commence. This concept will be briefly expanded upon in Chapter 2.

The presence of CO_2^* is important since the isotopic exchange between the DIC species and water occurs through carbonic acid. Kim et al. (2006) found that CO_3^- ions are preferentially incorporated into the precipitating $CaCO_3$ and that the other species will only be integrated after deprotonation. However, each species has a unique isotopic composition which can be reflected in the isotopic signature of the CO_3^{2-} if insufficient time is given for re-equilibration. As observed in their studies of planktonic foraminifera, both Sparo et al. (1997) and Zeebe (1999) illustrate that the $\delta^{18}O$ in calcite decreases as CO_3^{2-} concentration (or pH) increases, however these studies described biogenic carbonates and their precipitation mechanism differs from abiotic precipitation. This is because the dominant DIC species at higher pH values become isotopically lighter as pH rises (for instance, CO_3^{2-} is lighter than HCO_3). However, Deines et al. (2005) reported that pH had no influence of the isotopic composition if the carbonate precipitates slowly. It is only through rapid precipitation that pH can influence the isotopic composition of the carbonate.

1.1.1 The Influence of Kinetic Effects

Given and Wilkinson (1985) noted that composition of precipitated calcite is controlled by the kinetics of surface nucleation and the amount of reactants, primarily carbonate ions, at

growth areas. Kim et al. (2006) found that CO_3^{2-} is preferentially incorporated into the crystal lattice and that, HCO_3^- can gradually deprotonate into CO_3^{2-}. This is due to the preferential dissociation of the lighter isotopologues of HCO_3^-. The newly formed CO_3^{2-} will carry the isotopic signature of the HCO_3^- until it has re-equilibrated with the water. The isotopic fractionation factor of the DIC is influenced by which species is present at a given pH.

Beck et al. (2005) examined the oxygen isotope fractionation factor and exchange between DIC species (HCO_3^-, CO_3^{2-}, and CO_2^*) and water at 15, 25 and 40 $^\circ$C. The study found that pH has a significant effect on the $\delta^{18}O_{DIC}$ and that this value can vary by 17 ‰, regardless of temperature. Beck et al. (2005) established that, at 25 ^{o}C, the $1000\ln^{18}\alpha_{(CO_3^{2-}\text{-}H_2O)}$ and $1000\ln^{18}\alpha_{(HCO_3^-\text{-}H_2O)}$ values were 31.00 ± 0.15 ‰ and 24.19 ± 0.26 ‰ respectively. These values are similar to those found by Kim et al. (2006) which reported a $1000\ln^{18}\alpha_{(CO_3^{2-}\text{-}H_2O)}$ value of 30.53 ± 0.08 ‰ and a $1000\ln^{18}\alpha_{(HCO_3^-\text{-}H_2O)}$ value of 23.71 ± 0.08 ‰ at the same temperature. Therefore, a $CaCO_3$ precipitate, which forms at 25 ^{o}C, will usually have a fractionation factor somewhere between these two values. It is also worth mentioning that, like the $BaCO_3$ from Beck et al. (2005), some of the carbonates from the thesis experiments precipitated so quickly during the initial stage of their precipitation that they retained the oxygen isotope composition of the DIC, which had been enriched due to the production of $CO_{2(aq)}$ as a result of $CaCO_3$ precipitation. This is because the system was not given enough time to equilibrate with the water before the crystals formed.

As proposed by Zuddas and Mucci (1994) and Kim et al. (2006), the precipitation rate is another factor which can influence the $\delta^{18}O$ value of a carbonate precipitate. High precipitation rates result in kinetic effects (which are a function of solution chemistry, pH and/or precipitation rate) primarily determining the isotopic composition, causing disequilibrium. In nature, the

influence of these factors depends on the level of $CO_{2(g)}$ degassing and evaporation within the system and whether the carbonates precipitate in an open or closed environment. If the precipitate forms slowly, it isotopically exchanges with the water over a period of time until it reaches isotopic equilibrium. For instance, as shown in Kim and O'Neil (1997), the isotopic composition of calcite at equilibrium between carbonate and water occurs at 28.3 ‰ (using the acid fractionation factor presented in Kim et al. (2007)). Therefore, if given enough time, the calcite will gradually change its isotopic composition until it reaches this oxygen isotope equilibrium value. However, if a precipitate forms quickly and is not given sufficient time to achieve isotopic equilibrium with its environment; it attains an isotopic composition which can vary depending on the carbonate species located closest to the area of nucleation. Gabitov et al. (2012) found that a high growth rate causes depletion in ^{18}O within calcite, whereas a slow growth produced a $\delta^{18}O$ value of calcite which was closer to the isotopic equilibrium value. It should also be noted that in addition to changes in pH, a change in temperature will also directly impact isotope exchange kinetics and thus the time required to achieve isotopic equilibrium. Under mid- pH conditions, rapidly precipitating carbonates will yield a calcite-water oxygen isotope fractionation factor closer to the oxygen isotope equilibrium value between bicarbonate and water of 31.00 ± 0.15 ‰. In this situation, the bicarbonate ions, which have been deprotonated into carbonate ions, were given insufficient time to attain oxygen isotope equilibrium between HCO_3 and CO_3^{2-} and therefore still carry the isotopic signature of HCO_3^-, despite being CO_3^{2-} ions. Similarly, a rapidly precipitated carbonate could have a permil fractionation factor ($1000\ln^{18}\alpha_{calcite\text{-}water}$) closer to that between $CO_3^{2-}$and H_2O of 24.19 ± 0.26 ‰ if it forms under higher pH conditions because more CO_3^{2-} is available for incorporation into the crystal lattice (versus that at lower pH).

1.2 Defining Isotopic Equilibrium

1.2.1 Isotopic Equilibrium Value between Calcite and Water

One of the first studies to assess the oxygen isotope fractionation factor between carbonate and water was O'Neil et al. (1969), which examined the oxygen equilibrium fractionation factors between alkaline-earth carbonates, including calcium carbonate, and water between 0 to 500ºC. The curve generated from this study is in general agreement with the findings of Kim and O'Neil (1997) for temperatures of 25ºC or above, however the oxygen fractionation factors begin to considerably deviate below this point. Kim and O'Neil (1997) contended that their fractionation factor curve is more reliable, citing numerous reasons including their certainty that only calcite precipitated and there was no influence from on the calcium carbonate polymorphs and the similarity of their curve to biogenic carbonates. The $1000\ln^{18}\alpha_{calcite\text{-}water}$ proposed by Kim and O'Neil (1997) can be determined by an expression (Equation 1) which encompasses the variables of calcite formation for low temperatures of 10 – 40°C. The equation is shown below:

$$1000\ln^{18}\alpha_{calcite\text{-}water} = 18.03\ (10^3\ /T) + 32.42 \quad \text{(Equation 1)}$$

Kim et al. (2007) reported that, at 25 ºC, a positive oxygen isotope fractionation factor of approximately 0.8 ‰ can be obtained between aragonite and calcite.

1.2.2 Controversy Regarding True Isotopic Equilibrium between Calcite and Water

The technique used by Kim and O'Neil (1997) to determine oxygen isotope equilibrium is widely used in other studies, including Romanek et al. (1992). However, in its study of Devil's Hole cave in Nevada, Coplen (2007) discovered natural samples which were known to be near oxygen isotope equilibrium. Unexpectedly, the oxygen isotope fractionation factor between the cave calcite and water at 33.7 ºC was found to be 29.8 ± 0.13 ‰, which corresponds to a $1000\ln^{18}\alpha_{calcite–water}$ value of 29.80 at 25 C. This value is significantly larger than the equilibrium

value of 28.3 ‰ reported by Kim and O'Neil (1997). Since the geochemical environment within the cave was deemed to be consistent for the last 10,000 years, Coplen (2007) concluded that the equilibrium fractionation factor proposed by Kim and O'Neil (1997) must be underestimated for temperatures between 5 and 40 ^{o}C. The experiments of Dietzel et al. (2009) support the claim of Coplen (2007) and state that kinetic effects had influenced the results of previous studies. However, it is worth mentioning that Dietzel et al. (2009) did not allow the establishment of equilibrium between DIC and water prior to their experiment. Additionally, using clumped isotope thermometry, Kluge et al. (2014) found that, the mean temperature at Devil's Hole was 30.6 ± 2.6 ^{o}C, which could explain ~0.6 ‰ of the variation between Kim and O'Neil (1997) and Coplen (2007). The study then concluded that the main reason for this difference is due to the relatively fast precipitation rate of the laboratory experiments compared to that of the Devil's Hole sample. However, the current status of clumped isotope thermometry is imperfect due to factors such as poor analytical resolution and a large standard deviation which may affect the sensitivity of Δ_{47} measurements. Thus, the debate continues and more thorough studies to need to be completed to evaluate each of these kinetic effects systematically.

Dietzel et al. (2009) studied the oxygen isotope fractionation factor of inorganic calcite precipitation at pH between 8.3 and 10.5, precipitation rates between 1.8 and 4.4 μmol $m^{-2}h^{-1}$, and temperatures of 5, 25, and 40 ^{o}C using a CO_2 diffusion technique (Figure 1.1). They stated that precipitation rate is influenced by pH and temperature. It was found that there is a linear relationship between apparent $1000\ln^{18}\alpha_{calcite\text{-}water}$ and the precipitation rate when temperature and pH are held constant. Additionally, the trends showed a negative relationship, with $1000\ln^{18}\alpha_{calcite\text{-}water}$ decreasing with increasing precipitation rate and, under disequilibrium conditions, elevated pH. The article described the accepted belief that the $\delta^{18}O$ values may not

truly reflect formation temperature since it can be influenced by non-equilibrium isotope effects caused by factors like solution chemistry, pH and/or the precipitation rate, as mentioned in Kim and O'Neil (1997) and Kim et al. (2006). The study noted the presence of kinetic effects even at slow precipitation rates within the lab and thus supports the claim of Coplen (2007). Dietzel et al. (2009) also stated that there are discrepancies regarding the interpretation of non-equilibrium isotope effects and which equilibrium values should be accepted. For instance, in natural carbonate samples, the $\delta^{18}O$ value can be influenced by growth rate, with rapid growth resulting in a lower $\delta^{18}O$ value. The article specified the measured oxygen isotope fractionation factors given in articles, such as Kim and O'Neil (1997), for precipitates growth at slow rates were incorrectly assumed to be at equilibrium and that surface entrapment of CO_3^{2-} is a valid model for isotopic fractionation factor during inorganic calcite precipitation. However, since the samples produced by Dietzel et al. (2009) did not allow the time for initial equilibrium between DIC and water and are thereby in a state of disequilibrium, it is difficult to truly determine the contributing factors.

Dietzel et al. (2009) stated that

> "Although Kim et al. (2006) claimed that the measured oxygen isotopic fractionation factors in the slow precipitation experiments were statistically indistinguishable; the precipitation rate effect might be actually noticeable in their experiments. In spontaneous precipitation, initial supersaturation is usually relatively high, then decreases with time, and finally reaches a constant value if the injection rate was constant. Therefore, the average precipitation rate of each experiment generally decreases with the experimental duration time. As shown in Fig. 6, the measured oxygen isotopic fractionation factors increase with the experimental duration time (h) in the slow aragonite precipitation

experiments of Kim et al. (2006) done at the same (Fig. 6a) or almost the same experimental condition (Fig. 6b). This indicates that even in the slow precipitation experiments of Kim et al. (2006), the measured oxygen isotopic fractionation factors might still be influenced by the precipitation rate".

However, upon comparing the data from the three samples mentioned in Dietzel et al. (2006) from Kim et al. (2006), the points only vary by a maximum difference of 0.35 ‰ (calculated by subtracting the lowest possible value for the first point from the highest possible value from the final point presented). Therefore, while a trend could be suggested using the aforementioned Figure 6 from Dietzel et al. (2009), the difference between the maximum and minimum values is too small to truly infer one. It is more likely that the difference is caused by simple human error than the influence of any known mechanism. Additionally, it is worth mentioning that Dietzel et al. (2009) excluded two samples provided in Kim et al. (2006) which precipitated under the same trend as the three that were included in Figure 6a. Before the addition of these two neglected points, a linear trend could be suggested based on the evidence presented in Dietzel et al. (2009) (as illustrated by the dotted line in the figure below). However, once these two points are included, a new trend arises (as shown by the solid line). At 100 hours, the $1000\ln{}^{18}\alpha_{\text{aragonite-water}}$ is at 28.95 ‰. The slope then increase at a constant rate until 216 hours passed, at which point the $1000\ln{}^{18}\alpha_{\text{aragonite-water}}$ is 29.01 ‰. The slope then suddenly increases for the next 189 hours as the $1000\ln{}^{18}\alpha_{\text{aragonite-water}}$ rises to 29.15 ‰. The slope then sharply declines from 405 to 451 hours as the $1000\ln{}^{18}\alpha_{\text{aragonite-water}}$ then increases by 6 ‰ to 29.21 ‰ (which is near the suggested equilibrium value for aragonite). The sudden changes in the slope for this new pattern cannot be explained by any known mechanism and thus is most likely not caused by a continued influence from precipitation rate. Instead, as mentioned above, it is more

plausible that this strange trend is caused by human error and that all five points are statistically indistinguishable. The trend illustrated in Figure 6 in Dietzel et al. (2009) also becomes less clear as points from similar experiments are added that were also neglected in the paper. Since some of these points occur outside of the range presented in Figure 6, the graph was recreated (Figure 1.1).

Gabitov et al. (2012) aimed to determine the effects of growth rate on oxygen isotope fractionation factor between calcite and water in high ionic strength solutions. They monitored the growth rate of calcite crystals by injecting different rare earth elements (REE) spikes at various periods during growth, which were incorporated into the crystals. This allowed for direct examination of individual growth intervals in their samples as well as determination of growth rates. The precipitates were then subjected to Secondary Ion Mass Spectrometry (SIMS) for $\delta^{18}O$ analysis. It was found that oxygen isotope fractionation factor between calcite and water increased from the center of the crystals towards the edge of the crystal, with growth rates showing an opposite trend. The study concluded that $\delta^{18}O$ decreases with increasing growth rate since the rapidly-growth centers were depleted in ^{18}O relative to the slowly-growth edges. This is consistent with the growth entrapment model (GEM), which states that disequilibrium fractionation factor between elements is a result of elements and isotopes between a crystal and a growth medium, which is due to "capture" of a chemically and isotopically anomalous near-surface region during crystal growth. Capture, whether partial or complete is determined by the trade-off between diffusion and growth rate. The results found that the near-surface regions were depleted in ^{18}O relative to the lattice at equilibrium and that the slow growth of the $\delta^{18}O$ value is close to the predicted value of Zeebe (2007) and those found by Coplen (2007). This lead them to conclude that CO_3^{2-} is one of the main sources of $\delta^{18}O$ in calcite and that faster

239 precipitation rates result in a greater amount of CO_3^{2-} being captured. However, the capture rate
240 of CO_3^{2-} from this study was slower than that of Dietzel et al. (2009). This could be due to three
241 possible explanations: rapid consumption of CO_3^{2-}, the insufficient time given to achieve
242 equilibrium, or that the growth rate was not high enough for 100% capture of ^{18}O from CO_3^{2-}.
243 Kluge et al. (2014) used clumped isotope thermometry to test the alternate equilibrium
244 value proposed by Coplen (2007). This proxy was used since it is uninfluenced by the water
245 composition and thus gives independent temperature estimates when carbonates form at
246 thermodynamic and isotopic equilibrium. The study analyzed eight mammillary calcite samples
247 from Devil's Hole and took four to eight measurements which found that the study period had a
248 constant Δ_{47} value. Moreover, the study found that the paleotemperatures for water in Devil's
249 Hole were constant at 30.6 ± 2.6 ºC between 27 to180 thousand years ago, despite the occurrence
250 of glacial and interglacial cycles. Kluge et al. (2014) also stated that it is unlikely, though
251 possible, that temperatures changed significantly since the last mammillary calcite precipitated
252 4,500 years ago and that $\delta^{18}O$ values were unaffected by growth rate effects. The offset between
253 the temperature derived from the Δ_{47} and the temperature of 33.7 ºC directly measured by
254 Plummer et al. (2000) and used by Coplen (2007) could explain only ~0.6 ‰ of the 1.5 ‰ offset
255 between the oxygen isotope fractionation factor determined by Kim and O'Neil (1997) and
256 Coplen (2007). The groundwater temperature also remained constant at 32.8-34.3 ºC. The study
257 concluded that the similarity to expected calibration data between clumped isotope data and
258 values from modern groundwater temperatures show that the calcite in Devil's Hole precipitated
259 in equilibrium. Deviations from the commonly used equilibrium calibrations were not only
260 detected in natural samples, but also in those precipitated in laboratory experiments (Dietzel et
261 al., 2009; Gabitov et al., 2012; Watkins et al. 2013). It was argued that laboratory experiments

show a growth-rate dependence of the fractionation factor, with a lower oxygen isotope fractionation factor between water and calcite at high growth rates (this is observed in Gabitov et al. (2012) where a $\delta^{18}O$ difference of 1.5 ‰ was observed between the samples grown close to equilibrium and the quickly precipitated ones). Therefore, this study concluded that laboratory time scales are too fast (~2 orders of magnitude faster than Devil's Hole of ~0.7μm/a) to truly reflect equilibrium and that this fast growth results in the preferential incorporation of ^{16}O into the calcite.

Affek and Zaarur (2014) precipitated $CaCO_3$ using the passive $CO_{2(g)}$ degassing technique and examined the oxygen and clumped isotope effects. They bubbled 100% $CO_{2(g)}$ into 1 L of deionized water for ~1 hour and added an undisclosed amount of reagent grade $CaCO_3$, with continuous stirring and bubbling for another hour. The remaining undissolved solids were then filtered and the remaining solution (200 mL) was placed into an Erlenmeyer flask. Most of the experiments were performed in pairs, with one flask containing solution being "loosely covered" by a watch glass to reduce evaporation and one being open to atmosphere. The precipitation and subsequent $CO_{2(g)}$ degassing at the solution surface mimics the processes involved in thin films that is characteristic of stalagmites. The authors found that the precipitates collected at the water's surface were ^{18}O enriched by approximately 1 ‰ compared to $\delta^{18}O$ of the carbonates found at the bottom of the solution. The surface $CaCO_3$ had precipitated in disequilibrium due to kinetic effects caused by $CO_{2(g)}$ degassing and was found to have a higher $\delta^{18}O$ and lower Δ_{47} relative to their calibration values. The study discovered that these offsets varied with temperature, with Δ_{47} values increasing and $\delta^{18}O$ decreasing as temperature rose. Contrary to theoretical predictions, this finding illustrates that there is a strong temperature dependent co-variance between $\delta^{18}O$ and Δ_{47} which suggests another mechanism which causes

additional fractionation factor between DIC and calcite in fast growing crystals. The study proposed that the observed trend may be the net result of processes with different isotopic effects that vary with temperature. These processes may be ^{18}O-enrichment in the DIC due to $CO_{2(g)}$ degassing which is countered by ^{18}O-depletion in the crystal relative to the DIC. $CO_{2(g)}$ degassing removes the lighter isotopes through the production of $CO_{2(g)}$, which causes the boundary layer between water and air to become supersaturated. Fractionation factor between calcite and DIC may be related to the growth rate which impacts the balance between attachment and detachment of carbonate ions to the mineral surface or the concentration of ^{16}O on the carbonate surface that is then incorporated into the bulk crystal. Regardless, the authors argue that the isotopic fractionation factor between DIC and calcite must be greater at lower temperatures to explain the observed ^{18}O trend.

The experiments of Affek and Zaarur (2014), despite being loosely fitted with a watch glass, can be considered open when compared to unpublished data from the McMaster Research Group for Stable Isotopologues (MRSI), which was sealed with a lid and tightly closed. The experiments performed by Affek and Zaarur (2014) with the watch glass fall along the same trend line as those performed without the watch glass, showing that the "loosely fit" watch glass had little to no effect on $\delta^{18}O$ or Δ_{47}. The open system conditions enhanced the $CO_{2(g)}$ degassing in the starting solution, leading to fast degassing at the surface and slow degassing at the bottom as the thickness of the solution increases, which drove carbonate precipitation at the surface and would have caused there to be a greater deviation from equilibrium and a greater loss in DIC. This trend would have been prominent at the water-air boundary and would have decreased towards the bottom of the flask until it plateaued at a certain depth. It is worth noting that the $CO_{2(g)}$ gradient for the experiments of Affek and Zaarur (2014) were unknown due to a lack of

information provided. The article mentioned that the growth rate for the carbonates which formed at the bottom of the flask was controlled by mass transport from the supersaturated surface layer and requires a lot of time, depending on the temperature of the solution (Beck et al., 2005).

1.2.3- The Impact of Carbonic Anhydrase (CA) on Kinetic Isotope Effects

Carbonic anhydrase (CA) is an enzyme which acts as a catalyst for the reversible CO_2 hydration and HCO_3^- dehydration reactions ($CO_{2(aq)} + H_2O \rightleftharpoons HCO_3^- + H^+$) (Lindskog et al., 1971; Pocker and Bjorkquist, 1977; Pocker and Sarkanen, 1978; Silverman and Vincent, 1984; Paneth and O'Leary, 1985), which the main pathway in which oxygen isotope exchange between the DIC and water occurs (Zeebe and Wolf-Gladow, 2001). CA works through metal ion catalysis, with the active site of this enzyme containing a zinc ion which bonds with the oxygen atom within a water molecule and lowers the pKa of water from 15.7 to 6.6 (Berg et al., 2002). This newly formed bond causes one H^+ proton to dissociate from the water molecule, causing it to form a hydroxide ion, which then allows for a nucleophilic attack on a carbon dioxide molecule, forming HCO_3^- (Berg et al., 2002). The instability of this molecule causes the enzyme to then displace the bicarbonate ion in favour of another water molecule, continuing this process. This cycle can be repeated up to a million times per second (Lindskog et al., 1997; Berg et al., 2002). This enzyme is utilized in a variety of natural processes which are vital for the metabolic processes of mammals, plants, and prokaryotes (Pocker and Sarkanen, 1978; Reed and Graham, 1981) and is contained within many calcifying organisms. The presence of this enzyme within the system greatly enhances the conversion of $CO_{2(aq)}$ and water to HCO_3^- and a liberated H^+ proton, a process which in the absence of the catalyst is considered rather slow. The reaction with the enzyme takes place typically ten thousand to one million (10^4 to10^6) times per second (Berg et al., 2002). Previous studies such as Uchikawa and Zeebe (2012), Watkins et al. (2013),

and Watkins et al. (2014) have shown that the presence of CA significantly reduces the oxygen isotope equilibration time between DIC and water and should thereby eliminate or reduce any kinetic effects within the CO_2-H_2O system, depending on the solution's pH and the quantity of CA used. This experiment aimed to utilize CA to examine the influence of kinetic effects within the studied system and possibly assist in discerning the value for oxygen isotopic equilibrium between carbonate and water.

1.4 Conclusion

The use of stable isotopes in carbonate minerals can help unlock our understanding of Earth's climate change since the establishment of isotopic equilibrium can reflect the formation environment. However, physicochemical factors such as kinetic effects cause the measured oxygen and carbon isotope fractionation factor to differ from true equilibrium between the carbonate and water. This reduces the resolution of current paleoclimate reconstruction. It is only through a thorough understanding of the climate history that current and future climate change can be predicted. The study of kinetic effects can also provide a better understanding of how various processes influence the isotopic fractionation factor within the carbonate system so that the magnitude of deviation from equilibrium can be better understood. Therefore, it is vital that oxygen isotope equilibrium between carbonates and water be studied so that the isotopic composition within carbonates can be accurately utilized by future researchers to better comprehend, appreciate, and model the fluidity of climate change and the interconnected influence these changes have on ecosystems, organisms, and humans alike.

1.5 Thesis structure

Chapter 1 of this manuscript provides a review of the necessary background literature in which this project builds upon. Chapter 2 describes the results of a kinetic isotope study which examines the influence of concentration, precipitation rate, and CO_2 degassing/production and

provides evidence in support the isotopic equilibrium between calcite and water as described in Kim and O'Neil (1997). The chapter also discusses the utilization of varying concentrations of carbonic anhydrase (CA) and its lack of influence on the oxygen and carbon isotope fractionation factor, suggesting that the carbonates precipitated so quickly that it prevented the system from attaining equilibrium even when CA was present. The conclusions of this thesis are presented in Chapter 4 and include both a summary of the research conducted as well as the candidate's specific contributions to our understanding of carbonate environments. The relevance and applicability of this research to the field geochemistry will be discussed, in addition to suggestions for future work, aimed at the new graduate student who wishes to continue in the field.

Appendix

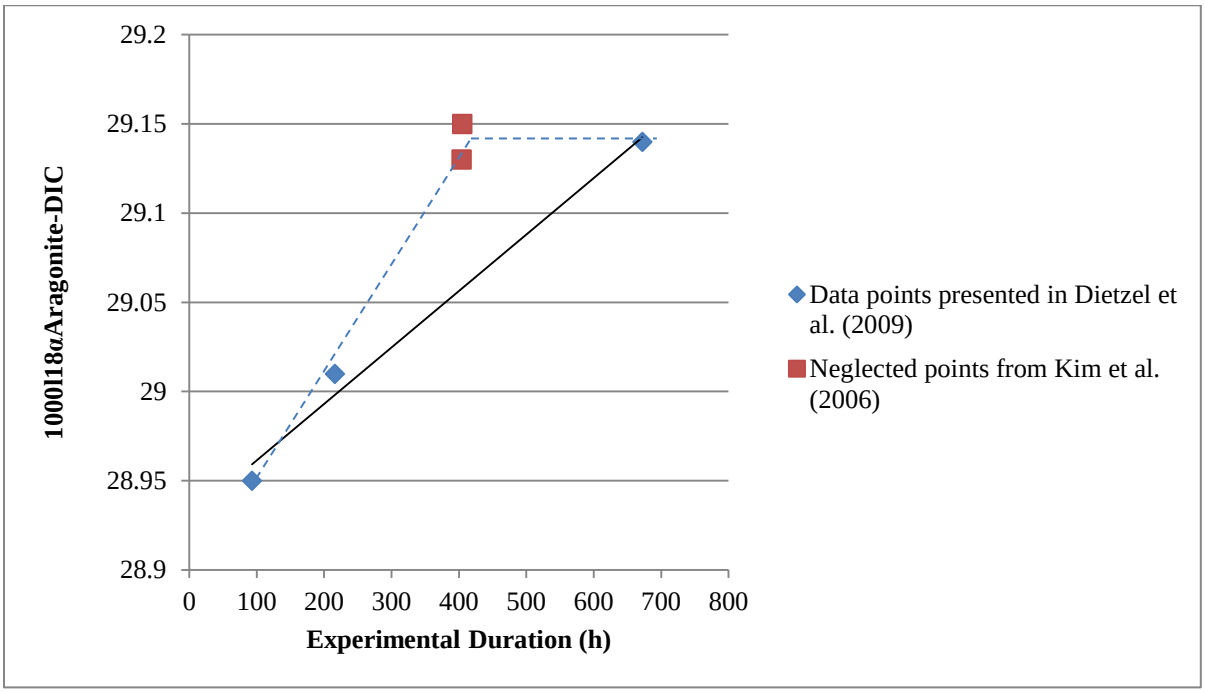

Figure 1.1. Figure 6 from Dietzel et al. (2009) after the missing points from Kim et al. (2006) were added.

References

Affek H. P. and Zaarur S. (2014) Kinetic isotope effect in CO_2 degassing: Insight from clumped and oxygen isotopes in laboratory precipitation experiments. *Geochim. Cosmochim. Acta* **143**, 319–330.

Beck W.C., Grossman E.L. and Morse J.W. (2005) Experimental studies of oxygen isotope fractionation factor in the carbonic acid system at 15 ºC, 25 ºC, and 40 ºC. *Geochimica et Cosmochimica Acta* **69**(14), 3493–3503.

Coplen T. B. (2007) Calibration of the Calcite-Water Oxygen-Isotope Geothermometer at Devils Hole, Nevada, a natural laboratory. *Geochimica et Cosmochimica Acta* **71**(16), 3948-3957.

Deines P. (2005). Comment on An explanation of the effect of seawater carbonate concentration on foraminiferal oxygen isotopes, by RE Zeebe (1999). *Geochimica et Cosmochimica Acta* **69**(3), 787-790.

Dietzel M., Tang J., Leis A. and Köhler S. J. (2009) Oxygen isotopic fractionation factor during inorganic calcite precipitation — Effects of temperature, precipitation rate and pH. *Chem. Geol.* **268**, 107–115.

Drever, James I. (1988) *The Geochemistry of Natural Waters, Second Edition. Englewood Cliffs, NJ: Prentice Hall. pp. 51–58.*

Epstein S., Buchsbaum R., Lowenstam H., and Urey H. (1953). Revised CarbonateWater Isotopic Temperature Scale. Geological Society of America Bulletin, 11, 1315–1326.

Gabitov R. I., Watson E. B. and Sadekov A. (2012) Oxygen isotope fractionation factor between calcite and fluid as a function of growth rate and temperature: An in situ study. *Chem. Geol.* **306-307**, 92–102.

Given R. K. and Wilkinson, B. H (1985) Kinetic control of morphology, composition, and mineralogy of abiotic sedimentary carbonates. *Journal of Sedimentary Petrology* **55**, 109-119.

Henry W. (1803) Experiments on the quantity of gases absorbed by water, at different temperatures, and under different pressures. *Phil. Trans. R. Soc. Lond. 93: 29–274.*

Kim S. and O'Neil J. (1997) Equilibrium and nonequilibrium oxygen isotope effects in synthetic carbonates. *Geochimica et Cosmochimica Acta* **61**(16), 3461–3475.

Kim S., Hillaire-Marcel C. and Mucci A. (2006) Mechanisms of equilibrium and kinetic oxygen isotope effects in synthetic aragonite at 25ºC. *Geochimica et Cosmochimica Acta* **70**, 5790-5801.

Kim S.-T., O'Neil J. R., Hillaire-Marcel C. and Mucci A. (2007) Oxygen isotope fractionation factor between synthetic aragonite and water: Influence of temperature and Mg2+ concentration. *Geochim. Cosmochim. Acta* **71**, 4704–4715.

Kluge T., Affek H. P., Dublyansky Y. and Spötl C. (2014) Devils Hole paleotemperatures and implications for oxygen isotope equilibrium fractionation factor. *Earth Planet. Sci. Lett.* **400**, 251–260.

Jimenez-Lopez C., Caballero E., Huertas F. J. and Romanek, C. S. (2001) Chemical, mineralogical and isotope behavior, and phase transformation during the precipitation of calcium carbonate minerals from intermediate ionic solution at 25 ° C. *Geochimica et Cosmochimica Acta* **65(19)**, 3219–3231.

Lindskog S. (1997). "Structure and mechanism of carbonic anhydrase". *Pharmacol. Ther.* **74** (1): 1–20.

Lindskog S. and Coleman J. E. (1973) The catalytic mechanism of carbonic anhydrase. *Proc. Natl. Acad. Sci. U. S. A.* **70**, 2505–2508.

McCrea J. M. (1950) On the isotopic chemistry of carbonates and a paleotemperature scale. *Journal of Chemical Physics* **18**(6), 849–857.

Paneth P. and O'Leary H. (1985) Carbon isotope effect on dehydration of bicarbonate ion catalyzed by carbonic anhydrase. *Biochemistry* **24**, 5143–5147.

Pocker Y. and Bjorkquist D. W. (1977) Stopped-flow studies of carbon dioxide hydration and bicarbonate dehydration in water and water-d2. Acid-base and metal ion catalysis. *J. Am. Chem. Soc.* **99**, 6537–6543.

Pocker Y. and Sarkanen S. (1978) Oxonase and esterase activities of erythrocyte carbonic anhydrase. *Biochemistry* **17**(6), 1110-1118.

Silverman D. N. and Vincent S. H. (1983) Proton transfer in the catalytic mechanism of carbonic anhydrase. *CRC Crit. Rev. Biochem.* **14**,207-255.

Spero H. J., Bijma J., Lea D. W. and Bemis, B. E. (1997). Effect of seawater carbonate concentration on foraminiferal carbon and oxygen isotopes. *Nature* **390**, 497–500.

Tarutani T., Clayton R. N. and Mayeda, T. K. (1969). The effect of polymorphism and magnesium substitution on oxygen isotope fractionation factor between calcium carbonate and water. *Geochimica et Cosmochimica Acta* **33**, 987–996.

Uchikawa J. and Zeebe R. E. (2012) The effect of carbonic anhydrase on the kinetics and equilibrium of the oxygen isotope exchange in the CO_2-H_2O system: Implications for $\delta^{18}O$ vital effects in biogenic carbonates. *Geochim. Cosmochim. Acta* **95**, 15–34.

Urey, H. C. (1947). The Thermodynamic Properties of Isotopic Substances. Journal of the Chemical Society, 562-581.

Watkins J. M., Nielsen L. C., Ryerson F. J. and DePaolo D. J. (2013) The influence of kinetics on the oxygen isotope composition of calcium carbonate. *Earth Planet. Sci. Lett.* **375**, 349–360.

Watkins J. M., Hunt J. D., Ryerson F. J. and DePaolo D. J. (2014) The influence of temperature, pH, and growth rate on the $\delta^{18}O$ composition of inorganically precipitated calcite. *Earth Planet. Sci. Lett.* **404**, 332–343.

Zeebe R. E. (1999) An explanation of the effect of seawater carbonate concentration on foraminiferal oxygen isotopes. *Geochimica et Cosmochimica Acta* **63**, 2001-2007.

Zeebe R. E. and Wolf-Gladrow D. A. (2001) CO_2 in seawater: equilibrium, kinetics, isotopes. *Elsevier Oceanogr. Ser.* **65**, 346.

Chapter 2:

Carbon and Oxygen Isotope Effects in Synthesized Calcite at 25 ºC

Chapter 2

"To raise new questions, new possibilities, to regard old problems from a new angle, requires creative imagination and marks real advance in science".

-Albert Einstein

2.1 Introduction

Carbonate environments have been abundant throughout Earth's history and the isotopic ratios of oxygen ($^{18}O/^{16}O$) and carbon ($^{13}C/^{12}C$) within carbonates can be utilized to deduce information about past environments, including temperature (Urey, 1947; Epstein et al., 1953; Broecker, 1986; Lea et al., 2000) and types of vegetation (Wickman, 1952; O'Leary, 1981; O'Leary, 1988; Dawson et al. 2002; Staddon, 2004). This is because, under ideal conditions, the precipitating carbonates exchange isotopes with their formation environment until isotopic equilibrium is attained. Isotopic equilibrium describes the point where the attachment of isotopes between two substances (i.e. calcite and water) equals the rate in which they are leaving. However the true oxygen isotope equilibrium fractionation factor which represents this point is currently debated upon, with Kim and O'Neil (1997) proposing 28.3 ‰ (using the acid fractionation factor from Kim et al. (2007)) at 25 ^{o}C and Coplen (2007) arguing 29.8 ‰. This information is important since it allows scientists to gain a better understanding of ocean temperatures and has broader implications regarding Earth's climate system and thus global warming. However, utilization of both oxygen and carbon isotopes in carbonate minerals and the aforementioned climatic information is obscured by "non-equilibrium isotope effects" in carbonates which are often affected by factors, such as solution chemistry, vital effects and precipitation rate (McCrea, 1950; Tarutani et al., 1969; De Villiers et al., 1995; Kim and O'Neil, 1997; Spero et al., 1997; Zeebe, 1999; Jiménez-López et al., 2001; Kim et al., 2006). Any sudden change in any of these factors will impact the isotopic exchange kinetics and thus the time

required to reach isotopic equilibrium. The isotope exchange between carbonates and water could further be influenced by the presence of dissolved aqueous carbonate species (Mills and Urey, 1940; McCrea, 1950; McConnaughey, 1989; Zeebe 1999; Kim et al. 2006; Zeebe, 2007) as well as the surface entrapment of CO_3^{2-} ions, which have varying impacts depending on pH and precipitation rate as found by Kim et al. (2006) and predicted by Deines (2005). Therefore, the goal of this research is to gain a better understanding of the influence of kinetic effects within the carbonate system. This will help to attain a greater understanding of oxygen isotope equilibrium and possibly help to determine which of the two proposed oxygen isotope fractionation factors truly represents isotopic equilibrium between calcite and water. This will assist in improving the use of carbonate minerals as paleotemperature proxies to help provide a stronger reference frame for future research about paleoclimate and the current observed changes in the global climate.

2.2 Methods

2.2.1 Preparation of Solution

Solutions were prepared by measuring the weights of varying concentrations of $NaHCO_3$ using a Sartorius® weighting scale. The solutes were then added to 1 liter of 18Ω deionized water, which was accurately determined through the use of a volumetric flask. Any surplus water was removed using a 100-1000 µm pipette and the remaining water was transferred into the glass Pyrex® media bottle. The caps of the bottles were then tightly sealed and covered with Parafilm® wax. All closed systems experiments conducted in this study were given this same treatment. Before each use, the bottles were placed within an acid bath containing approximately 5% hydrochloric acid (HCl) for a minimum of two days (depending on whether the bottles had been used before). The bottles were then rinsed twice using diluted water and twice using deionized water. The exterior of the bottles were then hand dried and the bottles were placed

within a 70 ^{o}C dryer for at least one day to remove any remaining water. Once prepared, the solutions were kept within a temperature chamber at 25 ± 0.1 ^{o}C for 7 days, a period which is significantly larger than 9 hour recommendation of Beck et al. (2005). Upon equilibration, the initial pH was then measured using an Oakton® pH electrode. The corresponding concentration of $CaCl_2$ was then added by dissolving $CaCl_2 \cdot 2H_2O$.

2.2.1.1 Normal Mixing Experiments (NM)

The definitions for all terms used in this manuscript can be found in Table 2.1. Three different closed bottle tests were performed to control the precipitation rate of the carbonates (Figure 2.1). The first, referred to as Normal Mixing Experiments (NM), added sufficient $NaHCO_3$ to produce solutions with concentrations of 5, 15, 25, and 50 mmolal to the deionized water and subsequently added an equimolar amount of $CaCl_2 \cdot 2H_2O$ after oxygen isotope equilibration between DIC and water had been established. Due to the hydrophilic nature of $CaCl_2$, all aliquots of the salt were weighed as quickly as possible and were discarded if the weighing time exceeded approximately one minute or water droplets were visible within the weighing dish. While this is potential source of error within this study due to the potential weighing offset caused the inclusion of water, it is not likely that this significantly influenced of the samples. This procedure was also replicated at 25 mmolal, but was left open to the atmosphere without the cap of the bottle. These experiments shall be referred to as the open, low ionic strength experiment.

2.2.1.2 Normal Mixing Experiments- Precipitation under an Open System

Solutions were also produced using the NM technique described above at a concentration of 25 mmolal under an open system and were given either six hours or one week to precipitate after the addition of $CaCl_2 \cdot 2H_2O$. The purpose of these experiments was to test the influence on

the isotopic composition as well as the morphological impact the open system may have on the crystal structure. The second set of samples were precipitated under saline conditions and were comprised of 5 mmolal of $NaHCO_3$, 10 mmolal of $CaCl_2 \cdot 2H_2O$, and 680 mmolal of NaCl or 5 mmolal of $NaHCO_3$, 67 mmolal of $CaCl_2 \cdot 2H_2O$, and 557 mmolal of NaCl. These carbonates were synthesized within a plastic container with dimensions of 41.4 cm length, 17.78 cm width, and 15.54 cm height (16.25 x 7.00 x 6.12 inches) which did not have a lid. This left ~736 cm^2 of water surface exposed to the atmosphere. The container was filled with 4 liters of deionized water and then stored in a growth chamber at 25 ± 0.1 ºC with a humidity of 95% for approximately one week.

2.2.1.3 Normal Mixing Experiments- High pH Solutions

Two groups of samples were also precipitated under high pH conditions (~11.07) through the reaction of Na_2CO_3 and $CaCl_2 \cdot 2H_2O$ at concentrations of 5, 15, and 25 mmolal. These solutions were prepared in the same manner as the Normal Mixing solutions precipitated under lower pH conditions. Beck et al. (2005) found that, at 25 ºC and at a pH of 11.7 and above, DIC requires 45 days to equilibrate with water. In contrast, according to Kim et al. (2006), those which form around ~10.7 require only 7 days. To test this, the first group was given one week to equilibrate after the addition of Na_2CO_3, as recommended by Kim et al. (2006), and the second group was given 50 days to equilibrate, in accordance with Beck et al. (2005). After the allotted time, $CaCl_2 \cdot 2H_2O$ was added to the solution and the system was given one week to precipitate before filtering. Solutions were always stored at 25 ± 0.1 ºC.

2.2.1.4 Partial Solid Addition (PSA) Experiments and Liquid/Liquid Mixing (LLM) Experiments

To reduce the carbonate precipitation time and attempt to obtain samples closer to isotopic equilibrium, a second set of samples, named the Partial Solid Addition (PSA) experiments, were precipitated using only concentrations of 5, 15, and 25 mmolal by adding

percentages of solid $CaCl_2 \cdot 2H_2O$ to a 1L solution of pre-dissolved $NaHCO_3$, over the course of three days (40% on the first day and 30% over the next two days) until the concentration of both chemicals were identical. A third set of closed system samples, known as the Liquid/Liquid Mixing (LLM) experiments, were prepared for the purpose of hastening the rate of precipitation. These experiments were prepared by pre-dissolving 5, 7, 10, 15, and 25 mmolal of $NaHCO_3$ and $CaCl_2 \cdot 2H_2O$ in individual 500 mL bottles and equilibrating the DIC for 5 days and storing both bottles at 25 ºC. After the allotted time elapsed, both corresponding 500mL solutions were subsequently poured into the same 1L bottle.

2.2.1.5 Experiments Catalyzed using Bovine Carbonic Anhydrase

Later experiments were then conducted using the NM and PSA experiments in the presence of three concentrations of carbonic anhydrase (CA) (purchased from MP Biomedicals - #153879). The first of these concentrations were based on the findings of Uchikawa and Zeebe (2012), which precipitated carbonates at a concentration of 15 mmolal and found that 1.9×10^{-5} mmolal was the most effective amount of CA used. To test the effects of CA in this study, CA concentrations of 0.63×10^{-5} mmolal and 3.17×10^{-5} mmolal were also selected, representing 1/3 and 1 2/3 of the concentration used in Uchikawa and Zeebe (2012). All three of these concentrations of CA were added to solutions containing 5, 15, and 25 mmolal of $NaHCO_3$ and eventually $CaCl_2 \cdot 2H_2O$ after equilibration at 25 ºC. Additional experiments were then conducted at a concentration of 38 micromolar, twice the amount used by Watkins et al. (2013), to further test the influence of CA on the system examined in this study. These experiments were only conducted at 15 and 25 mmolal due to the pH declining effect of CA which hindered significant crystal growth at 5 mmolal.

2.2.2 Storage of Solution in Constant Temperature

As mentioned above, after the addition of $CaCl_2 \cdot 2H_2O$, the caps of the bottles were tightly sealed by wrapping Parafilm® wax was around the cap and neck of the bottle. The first sets of mid-pH, NM solutions at concentrations of 5, 15, and 25 mmolal were maintained at 25 ± 0.1 ºC within the temperature chamber for 1, 3, 5, and 7 weeks. Over the designated time, the solutions were observed and the appearance of calcite rafts within each bottle was noted. All other solutions used in this study were stored at 25 ± 0.1 ºC for one week after the addition of $CaCl_2 \cdot 2H_2O$. In order to attain a greater accuracy, all of these experiments were performed three times at each condition. After the allotted time, the pH of the solutions were measured and compared to the initial pH (~8.2 for mid-pH experiments). Surface, or "raft", carbonates precipitated from most of the NM experiments were then collected using a hand-crafted miniature ladle.

2.2.3 Filtration of Solution and Collection of Samples

A vacuum filter was used in order to collect precipitate samples from the solutions. It was built by inserting a fritted glass funnel support with a silicone stopper into a 1 L Büchner flask. Type HVLP Durapore® filter paper with a pore size of 0.45µm was placed over top the membrane of the funnel support and moistened with deionized water. A 300 mL Büchner funnel was then positioned over the funnel support and secured with a clamp. A rubber hose was fitted over the hose barb of the Büchner funnel, which withdrew air from the flask, creating a vacuum.

A glass rod with a rubber policeman was then used to destabilize the precipitates from the sides and bottom from both sets of solution. The solution was poured into the Büchner funnel where the water filtered through the membrane into the flask, leaving only the precipitates on the filter paper. Deionized water followed by methanol was then poured into the Büchner funnel to ensure that all precipitates were deposited onto the filter paper. The filter paper was removed

and placed within a Petri dish. Deionized water was added to the now emptied bottle and the stir stick was then used to destabilize the precipitates from the bottom of the flask. The beaker with calcite raft precipitates was filtered in this same fashion. Once collected, the Petri dishes were placed into an oven at 70 ^{o}C for one day to remove any excess water. Afterwards, the samples were weighed using a Sartorius® scale and placed within small vials.

2.2.4 Stable Isotope Analysis

Samples of the precipitates were weighed using a Mettler Toledo® weighing scale and placed into small stainless steel sample cups. These cups were then placed into an ISOCARB automated acid bath at 90 ^{o}C (precision of ± 0.08 ‰) attached to a Fisions Optima® dual-inlet Isotope Ratio Mass Spectrometer (IRMS) to determine their isotopic composition. The carbonate samples were run against the standards NBS-19, NBS-18 and LSVEC. The solution and DIC samples were run using a Finnigan DELTAplusXP continuous flow stable isotope-ratio mass spectrometer (precision of ± 0.05 ‰). The solution samples were run using the lab standards MRSI W1 (0.58 ‰) and MRSI W2 (28.08 ‰) which had been previously calibrated against SMOW and SLAP. The δ^{18}O of the calcite was then calculated using the acid fractionation factor of 1.01030 as described in (Kim et al., 2007). The carbon isotope composition of DIC ($\delta^{13}C_{DIC}$) was run against NBS 18, NBS 19, and LSVEC and the percent composition of the DIC was attained by measuring lab DIC standards with known concentrations of 2, 5, and 8 mmolal, examining the area under the curve of the mass 44 peak, and comparing them to the measured samples. The data from both mass-spectrometers was then normalized to obtain the isotopic compositions. All of the calculated carbon isotope fractionation factors were calculated using the initial $\delta^{13}C_{(DIC)}$.

Some of the samples representing each condition were then sent to McMaster Analytical X-Ray Diffraction Facility (MAX) for X-ray diffraction (XRD) analysis.

2.3 Results

2.3.1 XRD Analysis and Decline in pH

The results of the XRD analysis showed that all samples precipitated under the closed system were composed of 100% calcite, regardless of concentration, technique, pH or whether CA was utilized. However, carbonates synthesized from low ionic strength solutions (i.e. without NaCl) in the open experiments yielded ~75 % calcite and ~25 % vaterite (Figure 2.2). In contrast, the carbonates precipitated from solutions of sea-water like ionic strength yielded 100% calcite, similar to the closed system experiments.

A trend can also be observed when examining the change in pH between initial and final conditions. It was found that pH always declined with increasing reactant concentration upon the addition of $CaCl_2$ (Figure 2.3). The addition of $CaCl_2$ always caused the pH to decline. In the mid-pH solutions, final pH was usually approximately 1, 1.6, 1.9, 2.3 units lower than under initial conditions for samples precipitated at 5, 15, 25, and 50 mmolal, respectively. For the high pH solutions, pH declined ~1.75 for 5 mmolal and ~2 for 25 mmolal samples. Speciation calculations found that the percentage of the isotopically heavy CO_2^*, which increases with acidity, grew with concentration from ~1.2 % under initial mid-pH conditions for all conditions to ~10, ~34, ~45, or ~66 % of the total DIC at 5, 15, 25, or 50 mmolal, respectively, under final pH conditions. Some of this available DIC was then incorporated into the synthesized $CaCO_3$. Similarly, the high pH samples increased from initial percent concentration of 0 % CO_2^* to 0.2 % at 5 mmolal and 1 % at 25 mmolal. Table 2.2 and Table 2.3 outline the typical DIC compositions of the samples synthesized in this study under initial and final conditions, respectively.

2.3.2 Uncatalyzed, Mid-pH Experiments

Approximately 83 individual experiments were conducted over the course of this study. Of these samples, 17 NM solutions had precipitates collected from the surface, side and bottom of the glass Pyrex® media bottle**.** All of the oxygen and carbon isotope compositions of the carbonates formed in this study are listed in Table 2.4 and 2.5. The $1000\ln^{18}\alpha_{(CaCO_3\text{-}H_2O)}$ values of all three closed, uncatalyzed, mid-pH experiments range from 28.43 to 29.8 ‰. In these experiments, the $1000\ln^{18}\alpha_{(CaCO_3\text{-}H_2O)}$ values of the 5, 15, and 25 mmolal NM samples had an average $1000\ln^{18}\alpha_{(CaCO_3\text{-}H_2O)}$ value of 28.88 ± 0.17, 29.17 ± 0.43, and 29.54 ± 0.22 ‰, respectively. All of these $1000\ln^{18}\alpha_{(CaCO_3\text{-}H_2O)}$ ranges are similar (i.e. within analytical error). The 50 mmolal samples had an average $1000\ln^{18}\alpha_{(CaCO_3\text{-}H_2O)}$ of 29.83 ± 0.03 ‰ and the 25 mmolal open bottle samples had an average value of 29.81 ± 0.03 ‰. Carbonates from the LLM experiments had average $1000\ln^{18}\alpha_{(CaCO_3\text{-}H_2O)}$ values of 28.93 ± 0.07, 28.65 ± 0.03, 29.91 ± 0.24, 29.58 ± 0.13, and 29.71 ± 0.13 ‰ for 5, 7, 10, 15, and 25 mmolal, correspondingly. The PSA experiments had $1000\ln^{18}\alpha_{(CaCO_3\text{-}H_2O)}$ values for the 5, 15, and 25 mmolal samples averaging from 28.52 ± 0.01, 29.09 ± 0.01, and 29.26 ± 0.06 ‰. The samples obtained from the open experiments had similar isotopic compositions to their closed system counterparts, with an average $1000\ln^{18}\alpha_{(CaCO_3\text{-}H_2O)}$ value of 29.81 ± 0.03 ‰. Due to the similarity of these samples to those which precipitated at the same concentration under a closed system, if any fractionation factor between vaterite and calcite occurred, it would have been minimal. These carbonates are the only ones in this entire study which precipitated vaterite.

Unfortunately the $\delta^{13}C$ of both the initial and final DIC of the NM experiments were not obtained and thereby no $1000\ln^{13}\alpha_{(CaCO_3\text{-}DIC)}$ values for the 5, 15, and 25 mmolal samples could

be accurately calculated. The $1000\ln^{13}\alpha_{(CaCO_3\text{-}DIC)}$ value of the 50 mmolal and 25 mmolal open system experiments averaged at 3.61 ± 0.38 and 3.62 ± 0.20 ‰, respectively. Samples from the LLM experiments obtained isotopic fractionation factor values for 5, 7, 10, 15, and 25 mmolal of 1.17 ± 0.06, 1.49 ± 0.20, 1.76 ± 0.09, 2.44 ± 0.44, and 2.23 ± 0.02 ‰, correspondingly. The carbonates from the PSA experiments attained values averaging from 0.62 ± 0.01, 2.71 ± 0.11, and 2.47 ± 0.33 ‰ for 5, 15, 25 mmolal, respectively.

2.3.3 Catalyzed Experiments

The $1000\ln^{18}\alpha_{(CaCO_3\text{-}H_2O)}$ of the calcite from the catalyzed experiments were identical to those of the uncatalyzed experiments, despite three different concentrations (i.e., 0.19, 0.57, and 0.95 mg/L) of carbonic anhydrase being used. The average oxygen isotope composition for all 5, 15, and 25 mmolal solutions were 28.51 ± 0.09 ‰, 29.22 ± 0.1 ‰, and 29.65 ± 0.02 ‰, respectively. The average $1000\ln^{13}\alpha_{(CaCO_3\text{-}DIC)}$ for each of the three concentrations using the PSA technique ranged from 1.74 ± 0.11 ‰, 3.21 ± 0.08 ‰, and 3.71 ± 0.10 ‰. Samples precipitated using the NM technique had compositions averaging from 1.91 ± 0.06 ‰ for 5 mmolal experiments and 3.91± 0.08 ‰ for those completed at 25 mmolal. However, samples precipitated in the presence of 0.38 μM (or 11.2 g/L) had a significantly lower $1000\ln^{18}\alpha_{(CaCO_3\text{-}H_2O)}$ and the $1000\ln^{13}\alpha_{(CaCO_3\text{-}DIC)}$ when compared to the uncatalyzed experiments precipitated using the same concentration of reactants (Table 5). The lower fractionation factor values of the catalyzed experiments cannot be explained by analytical error. Samples from the catalyzed 15 mmolal experiments had an average $1000\ln^{18}\alpha_{(CaCO_3\text{-}H_2O)}$ and$1000\ln^{13}\alpha_{(CaCO_3\text{-}DIC)}$ value of 28.95 ± 0.03 ‰ and 3.02 ± 0.02 ‰, respectively. The calcite precipitated at 25 mmolal in the presence of CA had an average $1000\ln^{18}\alpha_{(CaCO_3\text{-}H_2O)}$ value of 29.23 ± 0.07 ‰ and 3.75 ± 0.04 ‰ for $1000\ln^{13}\alpha_{(CaCO_3\text{-}DIC)}$ value. The oxygen isotope fractionation factor of the uncatalyzed, mid-pH

samples precipitated at the same concentration had a $1000\ln^{18}\alpha_{(CaCO_3\text{-}H_2O)}$ value of 29.59 ± 0.17 ‰ (0.36 ‰ difference) and a $1000\ln^{13}\alpha_{(CaCO_3\text{-}DIC)}$ value of 2.35 ± 0.24 ‰ (1.4 ‰ dissimilarity). Catalyzed experiments were not undertaken in the high pH system since the effectiveness of CA reduces with increasing pH (Roughton and Booth, 1946; Kernohan, 1964; Lindskog and Coleman, 1973; Donaldson and Quinn, 1974; and Berg et al., 2002). Therefore, it would no longer act as an effective catalyst and it is less likely to impact the isotopic fractionation factor within the faster precipitating high pH experiments.

2.3.4 High pH Experiments

All of samples from high pH experiments, regardless of whether they were equilibrated at 7 or 50 days, showed a $1000\ln^{18}\alpha_{(CaCO_3\text{-}H_2O)}$ trend which ran in the opposite direction as those precipitated at mid-pH, with 5 mmolal samples having a larger oxygen fractionation factor than 25 mmolal samples. The 5 mmolal samples had an average $1000\ln^{18}\alpha_{(CaCO_3\text{-}H_2O)}$ of 26.21 ± 0.06 ‰ and an average $1000\ln^{13}\alpha_{(CaCO_3\text{-}DIC)}$ of 0.23 ± 0.02 ‰ for the 7 and 50 day experiments, respectively. The 25 mmolal samples had averaged $1000\ln^{18}\alpha_{(CaCO_3\text{-}H2O)}$ of 25.10 ± 0.11 ‰ for 7 and 50 days. The average $1000\ln^{13}\alpha_{(CaCO_3\text{-}DIC)}$ value was 0.19 ± 0.03 ‰. The pH of these samples declined slightly after the addition of $CaCl_2{\cdot}2H_2O$.

2.4 Discussion

2.4.1 The Influence of pH Declined

As the pH declined over the course of calcium carbonate formation, the DIC speciation also changed and altered their carbon and oxygen isotope compositions within the DIC components. Due to the rapid precipitation rate of this system, there would have been little time available for isotopic re-equilibration of these DIC species after deprotonation into CO_3^{2-}, which is the species that is incorporated into the precipitating carbonate (Kim et al., 2006). Since the

degree in which this process occurred varied with concentration of $NaHCO_3$ and $CaCl_2$, the magnitude of this effect would have increased with the concentration of the reactants. The pH also declined in the high pH system, however this was strictly due to the liberation of H^+ protons from the water.

2.4.2 The influence of NaCl on Calcium Carbonate Morphology

The open system solutions precipitated through passive $CO_{2(g)}$ degassing in the presence of NaCl in this study always yielded 100 % calcite. This is due to the increased presence of ions from the dissolved NaCl which increased the calcite's solubility and delayed the precipitation of $CaCO_3$, causing the solution chemistry of the solution to prohibit the nucleation of vaterite (Takia et al., 2007). These results conflict with the findings of Kluge and John (2015), who precipitated 100 % vaterite at 23 ^oC in the presence of 6.4 M L^{-1} of NaCl (~10 times the amount used in this study). However, the study pre-dissolved pure calcium carbonate and precipitated samples by bubbling N_2 through the solution. This may have negated the aforementioned effect from sodium chloride since active $CO_{2(g)}$ degassing would have purged the system of $CO_{2(aq)}$ and increased the saturation state, causing the $CaCO_3$ to rapidly precipitate as vaterite.

2.4.3 Duration in the Uncatalyzed, Mid-pH Experiments

The duration the samples spent within the growth chamber after the addition of $CaCl_2{\cdot}2H_2O$ before filtration was also examined for possible isotopic effects within the NM experiments (Figure 2.4). It was found that there is no significant difference in the $1000\ln{}^{18}\alpha_{(CaCO_3\text{-}H_2O)}$ over the studied time periods, meaning that all of the carbonates formed within a week and did not continue to participate after initial formation.

2.4.4 *The Effect of Concentration and Precipitation Rate*

The quick reaction rate between the $NaHCO_3$ and $CaCl_2 \cdot 2H_2O$ is a major process governing the system since it would have introduced kinetic effects and prevented the isotopic equilibrium between $CaCO_3$ and water. This is because isotopic equilibrium requires both precipitation rate and CO_2 production to be slower than the time it takes for the carbonate-water system to buffer the impacts of kinetic effects (Beck et al, 2005; Kim et al., 2006; Coplen 2007; Dietzel et al., 2009; Gabitov et al, 2012; Watkins et al., 2013). The faster precipitation rate of the experiments conducted a higher concentration of initial reactants would have, as briefly discussed above, contained CO_3^{2-} ions which reflected an elevated isotopic signature from the HCO_3^- ions since they were not given enough time to isotopically re-equilibrate after deprotonation into the CO_3^{2-} ion. In contrast, the samples which precipitated at lower concentrations had more to time equilibrate isotopically and thereby have a lower oxygen isotope fractionation factor.

The higher concentrated solutions also precipitated a larger amount of $CaCO_3$ due to the solubility product (K_{sp}) of calcium carbonate, which ranges from 3.7×10^{-9} to 8.7×10^{-9} at a constant temperature of 25 °C, depending on the data source (Lide, 2005). As described above, the K_{sp} describes the amount of dissolved ions which can stay within the solution and that precipitation will readily occur once the K_{sp} is surpassed. Thus, as the concentration of initial reactants increases, more ions become available in the solution which cannot be remain in their dissolved state, promoting further precipitation of the solid $CaCO_3$. The rate in which this occurs increases with the amount of dissolved Ca^{2+} and CO_3^{2-} since the higher concentration creates a higher likelihood that the atoms of the reactants will collide with each other and start to precipitate (Chang and Goldsby, 2013). This influenced both carbon and oxygen in the system

and resulted in an enrichment trend. This is enforced by Table 2.4 which shows that the difference between the measured $1000\ln^{18}\alpha_{(CaCO_3\text{-}H_2O)}$ and $1000\ln^{13}\alpha_{(CaCO_3\text{-}DIC)}$ increases with concentration in all experiments. Therefore, it is certain that the 25 mmolal samples precipitated at a faster rate than those synthesized at 15 mmolal and so forth. This coincides with a visual inspection of when the carbonates first became visible to the naked eye.

2.4.5 Comparing the Data to Previous Research

The carbon and oxygen isotope fractionations in this study illustrate a positive linear trend with increasing reactant concentration (and thus precipitation rate and kinetic effects), which deviates away from the equilibrium oxygen isotope fractionation factor for 25 ^{o}C suggested by Kim and O'Neil (1997) and moves towards the one reported by Coplen (2007) (Figure 2.5). The strong correlation between δ^{13}C and δ^{18}O illustrates that the carbonates formed within a finite system. Since all of the carbonate samples were aged for a week before the addition of $CaCl_2$, it is believed that all of the experiments achieved oxygen isotope equilibrium between DIC and water and that the magnitude of deviation from this point is dependent on the amount of kinetic effects introduced through their varying precipitation rates. As mentioned above, all carbonates were fully formed within a short period of time (Figure 2.4). The carbonate samples obtained from 25 and 50 mmolal concentrations precipitated the quickest and all had $1000\ln^{18}\alpha_{(CaCO_3\text{-}H_2O)}$ values on or near the equilibrium fractionation factor proposed by Coplen (2007). This suggests that this value does not represent equilibrium. This supports the findings of Chacko and Deines (2008), who used theoretical calculations to obtain the oxygen isotope fractionation factor between calcite and water and also found that the equilibrium fractionation factor was "substantially larger" than what they had found. This study is further reinforced by the findings of Chacko et al. (1991), Kieffer (1982), and Schauble et al. (2006). If

the value proposed by Coplen (2007) truly represents equilibrium, then all contrasting empirical and theoretical data are incorrect. However, Chacko and Deines (2008) also stated that it cannot be unquestionably proven that the current water temperature and isotopic fractionations found in Devil's Hole remained the same since the sample analyzed by Coplen (2007) precipitated. While this cannot be confirmed either way, the similarity between the 25 and 50 mmolal samples precipitated in this study and the Devil's Hole carbonate suggest that the value suggested by Coplen (2007) is a natural barrier that the samples with the most kinetic effects could not penetrate (Figure 2.5 and 2.6). Both of these figures also illustrates that a similar natural barrier prevents the carbon isotopes from exceeding a certain point.

2.4.6 Isotopic Enrichment Due to Saturation Induced $CaCO_3$ Precipitation

The isotopic composition of calcium carbonate in this system may have also been influenced by CO_2 related processes, which can be caused by two processes. One is through the $CO_{2(g)}$ degassing induced precipitation caused by the pCO_2 gradient between the atmosphere and the water (which will be referred to as Type I carbonate precipitation mechanism from here onwards (Type I CPM)). The other is a consequence of $CO_{2(aq.)}$ (and some $CO_{2(g)}$) being produced as a by-product of the chemical reaction required to precipitate calcium carbonate (Type II CPM) in which $CO_{2(aq)}$ is produced by the dissociation of carbonic acid which formed through the reaction between a liberated H^+ proton and a free HCO_3^{2-}. As discussed above, Ca^{2+} reacts with HCO_3^- to produce $CaCO_3$ and H^+, these liberated H^+ protons can the react with some of the HCO_3^- in solution to form H_2CO_3 (carbonic acid). This molecule then dissociates in the presence of water to become carbon dioxide and water. This is described in the following reaction:

$$HCO_3^- + H^+ \rightleftharpoons H_2CO_3 \rightleftharpoons CO_{2(aq)} + H_2O$$

In general, both Type I and II cause an enrichment of the DIC layer due to the lighter isotopes of both carbon and oxygen being expelled in the form of CO_2 (either in gaseous or aqueous form) (Hendy, 1971; Usdowski and Hoefs, 1990; Mickler, 2004). This can cause all of the DIC species within the water to be ^{18}O and ^{13}C enriched (Kluge et al, 2014) and is why the carbonates precipitated at the air-water boundary in Affek and Zaarur (2014) were isotopically heavier than those which formed at the bottom of the flask. The high amount of $CO_{2(g)}$ degassing at the surface caused the carbonates to rapidly precipitate and introduced kinetic effects. In contrast, the bottom carbonates did not precipitate as quickly because the thick film of the solution reduced the rate of $CO_{2(g)}$ degassing and caused the carbonates to form at a slower rate through mass transport. This resulted in the carbonates being isotopically less heavy than the surface carbonates and thereby closer to isotopic equilibrium. While the relative magnitude of both enrichment processes in this study is unknown, it is likely that a similar process (Type II CPM) influenced this system.

The experiments described in this study were conducted in a closed system and any kinetic effects observed within the precipitated calcite due to Type II CPM would have prevented the aforementioned dual precipitation rate between the surface and bottom carbonates seen in Affek and Zaarur (2014). Since this study precipitated carbonates through chemical reaction, and not the pCO_2 gradient between atmosphere and water, all carbonates, regardless of location within the bottle, were equally influenced by the production of $CO_{2(aq)}$. Therefore, the surface, side and bottom samples all precipitated quickly and were isotopically influenced by CO_2 production through a chemical reaction and an equal amount of kinetic effects. This caused them to have an isotopic fractionation factor which was similar to the one observed in Affek and Zaarur (2014). It is for this reason that the samples collected from the surface, side and bottom

from this study had similar isotopic compositions (Figure 2.7). While no concentration information was given in Affek and Zaarur (2014), there was a similarity in the isotopic enrichment between the oxygen isotope fractionation factor of the surface samples at 25 ºC (28.54 and 28.84 ‰) and all of the carbonates precipitated at 5 mmolal in this study. This suggests that the increase in the $CO_{2(aq)}$ reservoir through Type II CPM might mimic the effects of $CO_{2(g)}$ leaving the solution through Type I CPM.

This process easily explains the carbon trend (since the DIC is the only carbon source in the system) and is described in Turner (1982) and Zhang et al. (1995), which state that $\delta^{13}C$ values of carbonate precipitates are determined by the degassing of $CO_{2(g)}$. The chemical bonds of these heavier isotopes are stronger compared to those composed of the lighter isotopes due to the reduced vibrational energy (and thus the zero point energy). This higher level of stability promotes the presence of isotopes with a higher atomic mass upon carbonate formation. Since the amount of vibrational energy within a system determines the activation energy, the lighter isotopes would have been incorporated into the initial $CO_{2(g)}$ created through Type I CPM and the heavier, more stable isotopes became integrated into the denser $CaCO_3$. Subsequent enrichment during carbonate precipitation was then caused by Rayleigh distillation. This is the only explanation that can be given at the current time which can explain the enrichment in carbon isotopes. It is unlikely that the rapid precipitation rate observed in the system can describe the carbon enrichment trend since the $1000\ln{}^{13}\alpha_{(CaCO3\text{-}DIC)}$ deviated from the carbon isotopic fractionation between HCO_3^- and calcite (~1 ‰ as described by Romanek et al. (1992)) as concentration of reactants (and the amount of DIC consumed) increased. If the faster precipitating samples incorporated a greater isotopic signature from the DIC, they would have approached 0 ‰ as the amount of consumed HCO_3^- grew, since there is only one carbon

reservoir in the system. Therefore, the faster precipitating carbonates could not have been incorporating the signature of the dominant DIC species at the pH in which it precipitated, meaning the carbon trend could not have been significantly influenced by the DIC.

This effect from Type II CPM also explains, at least in part, the oxygen trend (whose main reservoir is the formation water) in this particular system since the precipitation and $CO_{2(aq)}$ production rates would have outpaced the time required for isotopes to exchange between two phases. Therefore, the system was not given enough time to equilibrate with the water before the carbonates precipitated and hence retained the signature of the enriched DIC species. This process created the strong correlation of the aforementioned trend and can be great enough to counter the attachment of lighter isotopes caused by the rapid precipitation rate.

The use of the passive $CO_{2(g)}$ degassing technique is the simplest and most elegant way to precipitate calcium carbonates and most closely resembles the natural conditions in which carbonates form. However, caution must be exercised under certain conditions such as this study to precipitate $CaCO_3$ with the aim of obtaining isotopic equilibrium to avoid any kinetic effects over the course of $CaCO_3$ precipitation.

2.4.7 Rayleigh Distillation and Carbon Isotope Enrichment in these Experiments

While the aforementioned processes describe why the amount of heavier isotopes under initial conditions would have increased with concentration, the continued enrichment over the time as the system continued to degas CO_2 and form calcite can be explained through Rayleigh distillation. While this process influenced both oxygen and carbon in this system, carbon was the only isotope which was strictly affect by Rayleigh distillation. Figure 2.8 illustrates a Rayleigh distillation curve which shows that the production of calcite produced an exponential enrichment in the DIC reservoir as $CaCO_3$ continued to precipitate and the residual fraction of DIC declined. Guo et al. (2009) illustrated that kinetic isotope fractionation factors can result

from changes in the amount of DIC within an aqueous solution associated with CO_2 dehydration and dihydroxylation and thereby influence the isotopic composition of the carbonates which subsequently form. As stated in Guo et al. (2009) a Rayleigh distillation-based trend will occur if the precipitation rate outpaces the time required for re-equilibration with the formation water, which occurred in this system. This process is what caused the positive linear trend which was observed in carbon and oxygen isotope fraction factors. The closed system of this study is an ideal environment for Rayleigh distillation since the DIC reservoir was finite and the products did not re-react with the reactants after formation.

Since carbonates grow gradually over a period of time, the portion of the crystal which formed initially will have an isotopic composition that differs from those which precipitated later. In the case of higher concentrated solutions, which precipitated $CaCO_3$ more quickly, the first carbonates to precipitate would have had elevated isotopic fractionation factors which were further from equilibrium and those which formed later had fractionation factors which would have been closer to the value suggested by Kim and O'Neil (1997) (i.e. the lower barrier of the system). Thus, each individual isotopic fractionation factor presented in this study is not an individual point, but an average of an entire spectrum of isotopic fractionation factors which changed over the course of the experiment which is represented by an averaged value. The magnitude of this effect could have increased with concentration and may explain why the preliminary data at higher concentrations appear to suggest that the faster precipitating carbonates of this study plateaued at a certain point. The same process would have occurred at experiments synthesized using lower concentrations; however, this range would have been smaller since they had less of an influence from $CO_{2(aq)}$ production and thereby experienced a lower amount of kinetic effects during precipitation.

While the data from the synthesized carbonates from this study reflect two processes working in tandem with each other, the sample analyzed by Coplen (2007) grew at an extremely slow rate and therefore cannot be affected by the incorporation of HCO_3^- ions which were not given enough time to equilibrate with water after deprotonation. However, the secondary enrichment process caused by $CO_{2(g)}$ degassing/$CO_{2(aq)}$ production could influence a slow precipitating carbonate. As discussed above, the system described by Affek and Zaarur (2014) was influenced by Type I CPM and had a similar oxygen isotope fractionation factor to the 5 mmolal samples of this study, which were influenced, at least in part, by Type II CPM. Thus both Type I and II CPM have similar enrichment effects. The conditions observed at the air-water boundary in Affek and Zaarur (2014) are analogous to precipitation occurring within a thin film in cave carbonates which form in the vadose zone (Kluge et al., 2014), however the calcite sample analyzed by Coplen (2007) formed in phreatic conditions (Palmer, 2007) at a depth of more than 5 m above the current level of ~ 30 m (Szabo et al., 1994). According to Kluge et al. (2014), the Devil's Hole sample precipitated through the following reaction:

$$Ca^{2+} + 2HCO_3^- \rightleftharpoons CaCO_3 + CO_2 + H_2O$$

The production of CO_2 as a by-product proves that it is possible that the mammillary calcite studied by Coplen (2007) may have been influenced by Type II CPM. Given that Brown's Room, the chamber within Devil's Hole where the sample analyzed by Coplen (2007) was taken from, was isolated from the atmosphere and only had an air-filled area above the water's surface, the environment would have somewhat resembled the closed conditions in which this study precipitated samples. Thus even a slow precipitating carbonate could be influenced by kinetic effects introduced through Type II CPM due to the means in which it precipitated. If this is true, then the rate in which these samples formed is irrelevant. Since the samples from this study

which had been least affected by kinetic effects approached the value mentioned by Kim and O'Neil (1997), it suggests that 28.3 ‰ represents the lowest limit attainable in this system (i.e. equilibrium). Thus, it is not a question of whether laboratory timescales are sufficient to attain equilibrium, but rather, if $CO_{2(g)}$ degassing or $CO_{2(aq)}$ production influenced the system.

2.4.8 Catalyzed mid-pH Experiments

The enzyme bovine carbonic anhydrase (CA) was utilized in this study to expedite equilibration between DIC and water. It was believed that this may reduce the kinetic effects on the precipitating carbonates by changing the isotopic signature of the DIC before it was incorporated into the growing $CaCO_3$. The CA would hasten the re-equilibration of CO_3^{2-} ions which had deprotonated from HCO_3^- and also potentially convert some of the isotopically light $CO_{2(aq)}$ which was produced as a by-product from Type II CPM back into HCO_3^- via metal ion catalysis, causing some light isotopes to have a second opportunity to become incorporated into the carbonate. The presence of CA would have altered the signature of the DIC compared to the uncatalyzed experiments and hence influenced the oxygen isotope fractionation of the calcium carbonate.

A comparison of the oxygen and carbon isotope fractionation factors between the uncatalyzed NM and PSA experiments to those synthesized using low concentrations of CA illustrate that these samples all of the samples are approximately within analytical error of each other (with the exception of the 25 mmolal samples for the PSA experiments). This similarity could be because the precipitation rate and $CO_{2(aq)}$ production in this system always outpaced the equilibration time between DIC and water (Table 2.6 and Figure 2.9). The 25 mmolal PSA experiments which were catalyzed using low CA concentrations are close to the value suggested by Coplen (2007), however given that these were the fastest experiments which utilized CA, it is likely that this is merely coincidental and that some unknown factor is what caused this

deviation. Most of these low CA samples were synthesized using the PSA technique, which was deemed to have had the slowest precipitation rate of all the techniques used, as illustrated by the distinctively low $1000\ln^{18}\alpha_{(CaCO_3\text{-}H_2O)}$ and $1000\ln^{13}\alpha_{(CaCO_3\text{-}DIC)}$ values shown in Figure 2.6. Therefore, while no absolute precipitation rate was determined in this study, the similarity between the catalyzed and uncatalyzed PSA experiments suggests that even the slowest forming carbonates in the system grew rapid enough to prevent CA from having any effect (Figure 2.9).

Additionally, the 25 mmolal samples which were precipitated in the presence of 38μM of CA were closer to the equilibrium fractionation factor described by Kim and O'Neil (1997) and had a similar oxygen isotope fractionation factor (i.e. within analytical error) to the uncatalyzed experiments at the same concentration. This similarity further suggests that some kinetic effects must have still occurred, even at these concentrations of CA, since the $1000\ln^{18}\alpha_{(CaCO_3\text{-}H_2O)}$ did not further approach either of the values of Kim and O'Neil (19997) or Coplen (2007). This suggests that the precipitation rate and the enrichment due to Type II CPM are occurring extremely quickly and that, regardless of the concentration of CA used, it cannot establish oxygen isotope equilibrium in this system. However, the large variability in the 15 mmolal data may suggest the high CA concentration may start to influence the system as the precipitation rate approached that of the 15 mmolal samples.

The higher concentration of CA did not affect the $1000\ln^{13}\alpha_{(CaCO_3\text{-}DIC)}$ and cause the system to approach the carbon isotope equilibrium reported by Romanek et al. (1992) and Mook (2000). Interestingly, an isotopic analysis of the CA used in this study performed on a Costech Elemental Combustion System (ECS) 4010 found that the enzyme has a carbon isotope signature of ~ -13 ‰. However, given that the carbon atoms within this enzyme are only present within the

inactive sites and not the portion which interacts with the water molecule, it is unlikely that this secondary reservoir could influence the carbon reservoir.

While catalytic effects of CA are widely known to rapidly facilitate the interconversion of $CO_{2(aq)}$ and water to HCO_3^- and a liberated H^+ proton, it cannot establish equilibrium within fast participating carbonates such as speleothems. The presence of CA in mammals, plants, and prokaryotes are due to a family of at least five different genes believed to have been produced through convergent evolution (Hewett-Emmett and Tashian, 1996; Liljas and Laurberg, 2000). The enzyme is important for the metabolic processes of a variety of organisms, including carbonaceous species such as some corals (Furla et al., 2000; Moya et al., 2008; Bertucci et al, 2011; Tambutté et al., 2011) and possibly foraminifera (ter Kuile.,1989), as well as other aquatic organisms such as algae (Bowes, 1969; Badger, 1994; Raven, 1995; Sültemeyer, 1998; Aizawa and Miyachi, 1986; Moroney et al., 2001; Soto et al., 2006) and sponges (Hatch, 1980, Jackson et al., 2007; Voigt et al., 2014). It can therefore easily enter the carbonate system through a variety of ways. CA is also found in all types of plants (Bradfield, 1947; Lamb, 1977; Badger, 1994; Moroney et al., 2001; Tripp et al. (2001)) meaning that drip water in caves which passed through vegetation will also carry a signature from the enzyme. If either the precipitation rate or the amount of CO_2 degassing/production is slow enough and the concentration of CA is such that it hastens the equilibration rate, then the carbonates may precipitate in or close to isotopic equilibrium. However, similar to the surface samples of Affek and Zaarur (2014), the $CO_{2(g)}$ degassing along the thin film of water over a speleothem occurs rapidly, subsequently causing precipitation rate to also occur quickly. These processes then outpace the equilibration time and introduce the kinetic effects similar to what was observed in this study. Given that this study

utilized a large amount of CA and still observed these effects, it seems likely that the use of CA to obtain equilibrium has its limits.

2.4.9 Precipitation Amount and Percent Yield

While the carbonates precipitated in this study did not precipitate 100% of the DIC, they do help to point out the issues with identifying isotopic equilibrium between carbonate and water (Table 6). These samples may also call into question whether the value proposed by Coplen (2007) truly represents this elusive value or if it simply represents a natural barrier in which the isotopic composition of carbonates in this system had difficulty penetrating. The similarity between the 25 and 50 mmolal experiments further supports this claim since increasing the amount of precipitated DIC resulted in virtually no difference in the oxygen isotope fractionation factor.

2.4.10 Kinetic Effects in the High pH Experiments

Unlike the mid-pH conditions, $CO_{2(aq)}$ is not produced as a by-product under this system because calcium carbonate is formed through the double displacement between Na_2CO_3 and $CaCl_2$:

$$Ca^{2+} + CO_3^{2-} \rightleftharpoons CaCO_3$$

Thus the $1000\ln^{13}\alpha_{(CaCO_3\text{-}DIC)}$ values in these experiments did not show the aforementioned enrichment trend observed with the mid-pH samples. Instead, each concentration had a relatively similar carbon isotope fractionation factor (Figure 2.10).

In contrast, the $1000\ln^{18}\alpha_{(CaCO_3\text{-}H_2O)}$ values did not follow the trend seen in the mid-pH experiments (Figure 2.10). Instead, the oxygen isotope fractionation factor values decreased with increasing solution concentration, with 5 mmolal samples being close to the equilibrium value proposed by Kim and O'Neil (1997) and higher concentration incorporating CO_3^{2-} and

having a smaller isotopic fractionation factor which approached the fractionation factor line outlined by Beck et al. (2005) and Kim et al. (2006). This resulted in a negative linear correlation between the $1000\ln^{18}\alpha_{(CaCO_3\text{-}H_2O)}$ and $1000\ln^{13}\alpha_{(CaCO_3\text{-}DIC)}$ values. This observation is similar to what was described by Zeebe et al. (1999); however, these samples precipitated under the influence of kinetic effects and further build upon the conclusions of Deines (2005) and Kim et al. (2006) that pH only influences isotopic fractionation factor under non-equilibrium conditions. In this system, it is believed that the value suggested by Kim and O'Neil (1997) represents the upper limit of the system and the CO_3^- the lowest. While the mechanisms causing deviation from isotopic equilibrium between calcite and water may slightly vary from the mid-pH samples, the oxygen isotope fractionation factor of this system still illustrates that there is a greater amount of kinetic effects introduced into the system as the samples deviate from the value proposed by Kim and O'Neil (1997).

The increase in the saturation index from 2.83 to 3.59 observed with the rising concentration resulted in a faster precipitation rate than those seen in the mid-pH solutions (which did not exceed 2.49) (Table 2.2). Table 2.7 and 2.8, which illustrate the total amount of DIC precipitated in the system, show that up to 98 % of the DIC reservoir was consumed during the high pH, 25 mmolal experiments, an amount greater than any other experiment in this study. This higher amount of the dominant DIC species would have been incorporated within the growing carbonate. This prevented the isotopic composition from being limited by an isotopic barrier like the mid-pH samples were and provided a similar effect to the $BaCO_3$ experiments of Beck et al. (2005) and Kim et al. (2006). However, the precipitation rate of $BaCO_3$ is faster than that of the high pH samples and precipitated the full amount of DIC possible. Therefore, the oxygen isotope fractionation factor of those samples would have been closer to that of the CO_3^{2-}

ions than the samples precipitated in this study and thus had a $1000\ln^{18}\alpha_{(CaCO_3\text{-}H_2O)}$ value which closer reflected the isotopic signature of this ion (24.19 ± 0.26 ‰ for Beck et al. (2005) and 23.71 ± 0.08 ‰ for Kim et al. (2006)).

2.4.11 Equilibration Time in the High pH System

The difference between the data collected from the 7 and 50 day experiments for carbon as well as oxygen isotope fractionation factors are within analytical error (~0.2 ‰) and can therefore be considered to be similar to each other (Figure 2.11). If the differences were larger, then these experimental observations would imply that most of the oxygen isotope equilibration between DIC and water at this pH could not be completed within 7 days. In other words, the similarity between the 7 and 50 day data suggests that oxygen isotope equilibrium between DIC and water at the pH of this system (~11.07) can be attained within one week. This supports the equilibration time used in Kim et al. (2006), but contrasts that of Beck et al. (2005). Kim et al. (2006) utilized pH levels of 10.08 to 10.75 in their experiments, resulting in CO_3^{2-} being composed of 41.85 to 76.94% of the total DIC. Since the pH was around 11.07 in this study, the amount of CO_3^{2-} ranged from approximately 89.6 to 93.14% of the total DIC. In contrast, Beck et al. (2005) synthesized their carbonates at pH levels of 11.83, 11.87, and 12.20 in which CO_3^{2-} would have taken up a ~100% of the total DIC. This suggests that the time required for oxygen isotope equilibration between DIC and water might change at an exponential rate as near complete dominance of one carbon species over its counterparts is attained. This is due to the effect of CO_2 hydration and the facilitation of isotopic exchange between $CO_{2(aq)}$ and water, the rate of which decreases as the amount of the proton containing DIC species declines. Once CO_3^{2-} becomes dominant, this carbon species has to overcome a high energy barrier to continue isotopic exchange. The similarity in oxygen isotope equilibration time between this study and

Kim et al. (2006), despite the differences in speciation, suggests that the oxygen isotope equilibration time will remain somewhat stagnant as long as at least 10.4 to 6.86 % of the DIC is HCO_3^-, allowing some degree of CO_2 hydration to occur. Once CO_3^{2-} attains complete dominance, CO_2 hydration is not as fast as it could be at lower pH levels. It is for this reason that the effect of CA also decreases as pH rises (Watkins et al., 2013).

2.5 Conclusion

The findings of this research illustrate some of the processes which can influence the isotopic fractionation of carbonates precipitated out of equilibrium. Samples believed to have undergone the highest amount of kinetic effects have $1000\ln^{18}\alpha_{(CaCO_3\text{-}H_2O)}$ values which are close to the one analyzed by Coplen (2007), suggesting that the value proposed by Kim and O'Neil (1997) is closer to true equilibrium. These kinetic effects are believed to have been caused by a combination of both the incorporation of CO_3^{2-} ions which were not given enough to equilibrate after deprotonation and Type II CPM caused by the production of isotopically light $CO_{2(aq)}$. However, the magnitude of these effects in relation to each other is unknown. This study also proposes that the utilization of $NaHCO_3$ and $CaCl_2$- H_2O to precipitate carbonates in this system cannot be used to precipitate carbonates in equilibrium since the resultant chemical reaction naturally causes an isotopic enrichment of the DIC due to CO_2 production caused by Type II CPM. The amount of $CO_{2(aq)}$ production and precipitation rate under these conditions outpaced the equilibration time even in the presence of varying concentrations of CA, meaning that this catalyzing enzyme may not be able to establish equilibrium in fast growing carbonates such as speleothems.

The experiments conducted at high pH (~11.07) achieved equilibrium between DIC and water within 7 days as stated in Kim et al. (2006), which contrasts with the time found by Beck

et al. (2005). This might be due to the varying presence of CO_3^{2-} ions present at the differing pH levels. It was also found that, unlike the mid-pH system, the $1000\ln^{18}\alpha_{(CaCO_3\text{-}H_2O)}$ increased with decreasing concentration. It is unlikely that Type II CPM affected this system since $CO_{2(aq)}$ is not formed as a by-product of the reaction which produced these carbonates. Thus the oxygen isotope fractionation factors of the samples precipitated in these experiments were strictly due to the fast precipitation rate and the incorporation of isotopically lighter CO_3^{2-}, which was dominant at this pH. This caused a deviation from initial isotopic equilibrium between carbonate and water. The $1000\ln^{13}\alpha_{(CaCO_3\text{-}DIC)}$ did not change in this system with increasing concentration due to the lack of $CO_{2(aq)}$ production.

The findings of this study suggest that laboratory timescales are sufficient to establish isotopic equilibrium and that a slow precipitation rate does not guarantee that no kinetic effects occurred. The establishment of isotopic equilibrium is not strictly dependent on precipitation rate alone, but a combination of equilibration time, amount of CO_2 degassing/production, and precipitation rate. It is not whether the precipitation rate is fast or not, but rather if the precipitation rate and/or CO_2 degassing/production are faster than the time required for equilibration. If this is not the case, then any system, natural or artificial, can attain isotopic equilibrium.

Appendix

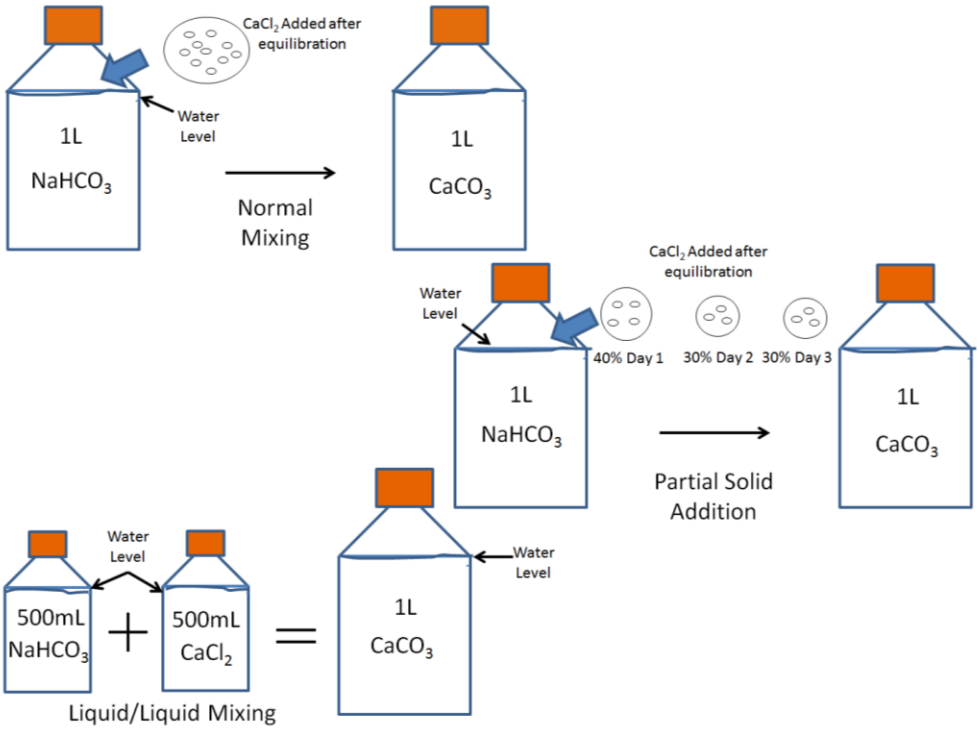

Figure 2.1. A basic outline of the three precipitation methods utilized in these experiments

Table 2.1. Abbreviated terms used in this manuscript

Term	Abbreviation
Oxygen Isotope Fractionation factor	$1000\ln^{18}\alpha_{(CaCO_3\text{-}H_2O)}$
Carbon Isotope Fractionation factor	$1000\ln^{13}\alpha_{(CaCO_3\text{-}DIC)}$
Normal Mixing	NM
Liquid/Liquid Mixing	LLM
Partial Solid Addition	PSA
Carbonic Anhydrase	CA

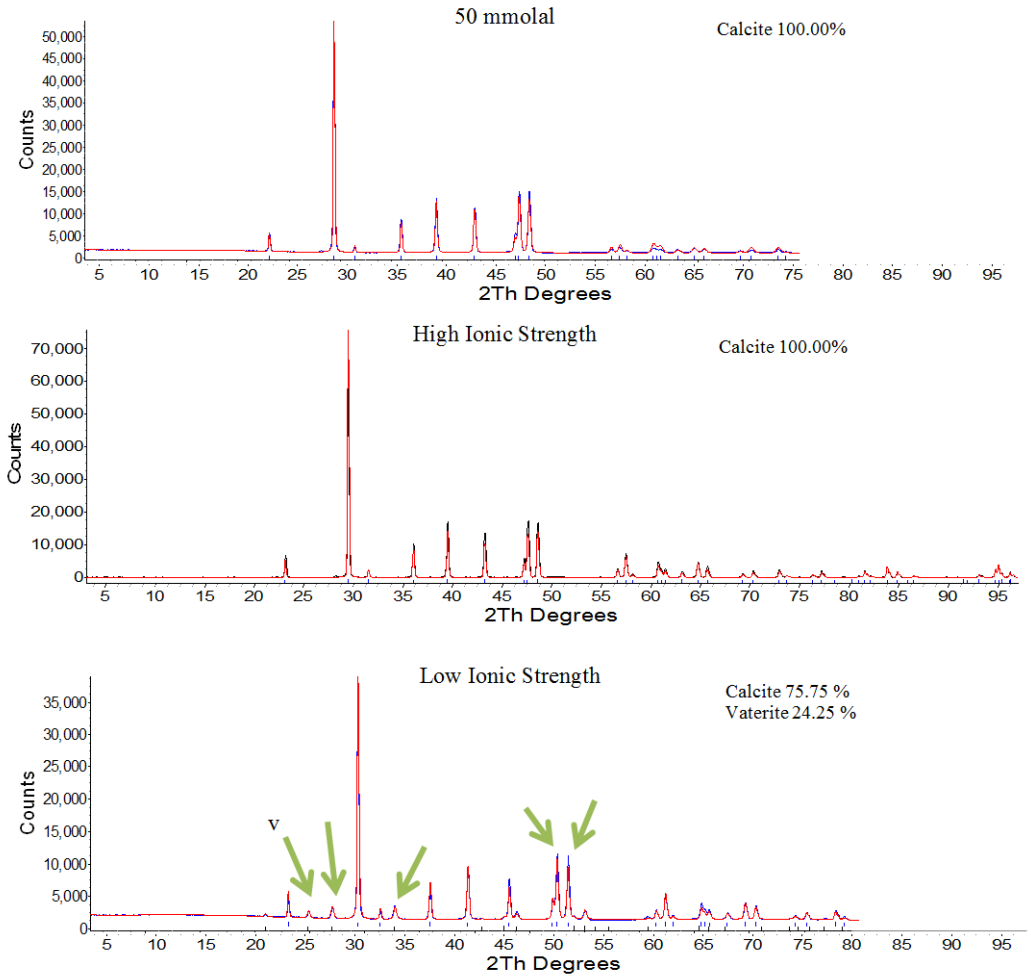

Figure 2.2. The results of the some of the XRD analyses performed in this study for the typical results for all closed experiments (A), the open experiments conducted under high ionic strengths (B), and the open experiments conducted under low ionic strengths without the presence of NaCl (C). The green arrows in (C) illustrate some of the XRD peaks which show the presence of vaterite within the system.

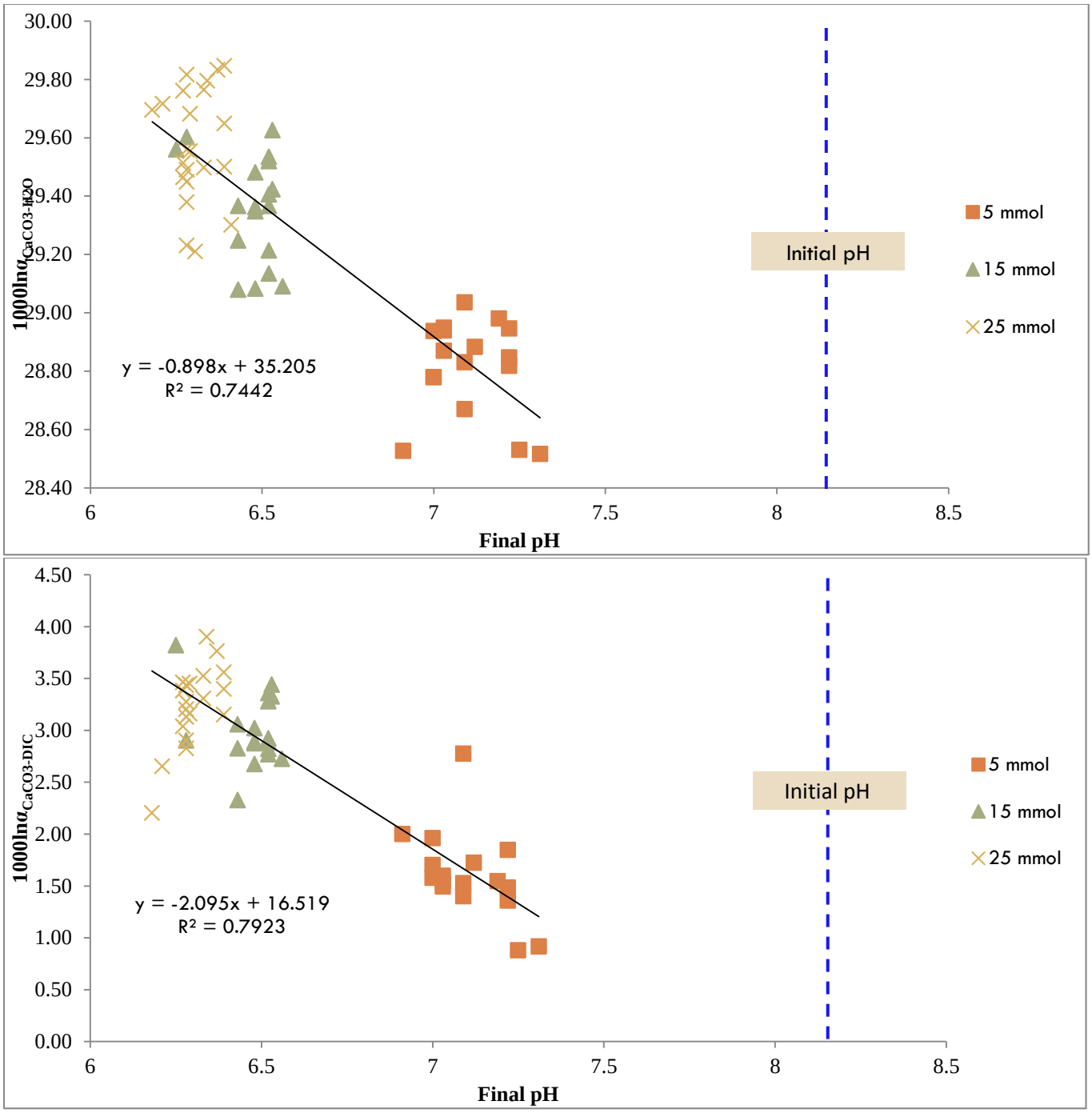

Figure 2.3. Relationship between oxygen isotope fractionation factor A) and carbon isotope fractionation factor (B) with final pH. The dashed line indicates the starting pH. It was found that pH declined as concentration increased.

Table 2.2. Typical speciation data for the initial conditions of experiments. The fractionation factors described below represent the point where each of the samples would have started. Initial pH represents the pH of the system after isotopic equilibrium between DIC and water was attained, but before the addition of $CaCl_2$.

Concentration	Initial pH	Saturation Index	Percent of DIC			Carbon Fractionation Factor (‰)	Oxygen Fractionation Factor (‰)
			CO_3^{2-}	HCO_3^-	CO_2		
5	8.2	1.4	0.97%	97.76%	1.28%	1.10	31.06
15	8.2	2.16	1.21%	97.57%	1.22%	1.09	31.03
25	8.2	2.49	1.39%	97.43%	1.18%	1.09	31.02
5	11.07	2.83	89.60%	10.40%	0.00%	0.45	24.81
15	11.07	3.35	91.99%	8.05%	0.00%	0.44	24.65
25	11.07	3.59	93.14%	6.87%	0.00%	0.43	24.57

Table 2.3. Typical speciation data for the final conditions of experiments. The increase in deviation for both carbon and oxygen for the mid-pH experiments illustrates the deviation from equilibrium with increasing concentration.

Experiment Type	Sample ID	Final pH	Concentration (mmolal)	$1000\ln^{13}\alpha_{(CaCO_3\text{-}DIC)}$	Diff. in $\delta^{13}C_{DIC}$ (Initial and Final)	$1000\ln^{18}\alpha_{(CaCO_3\text{-}H_2O)}$	Diff. in $\delta^{18}O_{H_2O}$ (Initial and Final)
Normal Mixing	MRSI-NR-2-1w-5c NM	7.22	5	N/A	N/A	28.82	0.03
	MRSI-NR-2-7w-5c NM	6.52	15	N/A	N/A	28.95	0.00
	MRSI-NR-2-1w-15c NM	6.52	15	N/A	N/A	29.25	0.01
	MRSI-NR-1-3w-15c NM	6.53	15	N/A	N/A	29.36	0.00
	MRSI-NR-1-3w-25c NM	6.28	25	N/A	N/A	29.82	0.02
	MRSI-NR-2-3w-25c NM	6.29	25	N/A	N/A	29.68	0.02
	MRSI-NR-1-50C NM	5.86	50	3.34	0.39	29.81	-0.01
	MRSI-NR-2-50C NM	5.91	50	3.88	0.21	29.85	-0.04
	MRSI-NR-1-25C-OB NM	6.34	25	3.76	-1.45	29.80	0.01
	MRSI-NR-2-25C-OB NM	6.37	25	3.48	-1.36	29.83	0.02
Partial Solid Addition	MRSI-NR-1-5C-PSA	7.25	5	0.63	-0.15	28.53	-0.03
	MRSI-NR-2-5C-PSA	7.31	5	0.61	-0.20	28.52	-0.03
	MRSI-NR-1-15C-PSA	6.48	15	2.79	-0.33	29.08	-0.04
	MRSI-NR-2-15C-PSA	6.56	15	2.63	-0.33	29.09	-0.03
Liquid/Liquid Mixing	MRSI-NR-1-5c-LLM	7.19	5	1.22	-0.08	28.98	0.00
	MRSI-NR-2-5c-LLM	7.12	5	1.13	0.18	28.88	-0.01
	MRSI-NR-1-7c-LLM	6.99	7	1.34	-0.06	28.63	-0.02
	MRSI-NR-2-7c-LLM	6.86	7	1.63	-0.45	28.67	0.01
	MRSI-NR-1-10c-LLM	6.65	10	1.70	-0.29	29.08	-0.01
High pH	MRSI-NR-1-5c-50d	10.32	5	0.23	1.40	26.20	-0.02
	MRSI-NR-1-25c-50d	10.72	25	0.19	1.85	25.22	0.01

Table 2.4. Experimental Data for Oxygen from Calcite.

Sample ID	Ca^{2+} and DIC conc.	pH	CA	$CaCO_3$ (mg)	$\delta^{18}O_{CaCO_3}$	$\delta^{18}O_{H_2O_{ini}}$	$\delta^{18}O_{H_2O_{fin}}$	$\alpha_{CaCO_3\text{-}H_2O}$	$1000\ln^{18}\alpha_{(CaCO_3\text{-}H_2O)}$
MRSI-NR-2-1w-5c NM	5	Mid	No	2	22.69	-6.46	-6.49	1.03	28.95
MRSI-NR-2-3w-5c NM	5	Mid	No	2	22.40	-6.45	-6.5	1.03	28.67
MRSI-NR-1-7w-5c NM	5	Mid	No	2	22.61	-6.54	-6.56	1.03	28.94
MRSI-NR-2-7w-5c NM	5	Mid	No	3	22.53	-6.64	-6.64	1.03	28.94
MRSI-NR-2-1w-15c NM	15	Mid	No	96	22.90	-6.54	-6.55	1.03	29.21
MRSI-NR-1-3w-15c NM	15	Mid	No	91	22.39	-6.53	-6.53	1.03	28.69
MRSI-NR-1-5w-15c NM	15	Mid	No	94	23.48	-6.39	-6.4	1.03	29.63
MRSI-NR-2-5w-15c NM	15	Mid	No	81	22.80	-6.51	-6.51	1.03	29.08
MRSI-NR-1-7w-15c NM	15	Mid	No	74	23.02	-6.56	-6.57	1.03	29.35
MRSI-NR-2-7w-15c NM	15	Mid	No	79	22.95	-6.47	-5.72	1.03	28.43
MRSI-NR-2-1w-25c NM	25	Mid	No	180	23.23	-6.49	-6.48	1.03	29.46
MRSI-NR-1-3w-25c NM	25	Mid	No	210	23.26	-6.52	-6.54	1.03	29.56
MRSI-NR-2-3w-25c NM	25	Mid	No	230	23.36	-6.48	-6.5	1.03	29.61
MRSI-NR-1-5w-25c NM	25	Mid	No	246	22.67	-6.45	-6.44	1.03	28.87
MRSI-NR-1-7w-25c NM	25	Mid	No	312	23.16	-6.54	-6.58	1.03	29.50
MRSI-NR-2-7w-25c NM	25	Mid	No	201	23.03	-6.46	-6.44	1.03	29.23
MRSI-NR-2-1w-5c NM	5	Mid	No	2	22.59	-6.46	-6.49	1.03	28.85
MRSI-NR-2-3w-5c NM	5	Mid	No	2	22.77	-6.45	-6.5	1.03	29.04
MRSI-NR-1-7w-5c NM	5	Mid	No	4	22.45	-6.54	-6.56	1.03	28.78
MRSI-NR-2-7w-5c NM	5	Mid	No	8	22.46	-6.64	-6.64	1.03	28.87
MRSI-NR-2-1w-15c NM	15	Mid	No	187	23.47	-6.54	-6.55	1.03	29.77
MRSI-NR-1-3w-15c NM	15	Mid	No	164	23.25	-6.53	-6.53	1.03	29.53
MRSI-NR-1-5w-15c NM	15	Mid	No	182	22.18	-6.39	-6.4	1.03	28.36

MRSI-NR-2-5w-15c NM	15	Mid	No	152	22.98	-6.51	-6.51	1.03	29.25
MRSI-NR-1-7w-15c NM	15	Mid	No	125	23.03	-6.56	-6.57	1.03	29.36
MRSI-NR-2-7w-15c NM	15	Mid	No	123	23.03	-6.47	-5.72	1.03	28.51
MRSI-NR-2-1w-25c NM	25	Mid	No	234	23.28	-6.49	-6.48	1.03	29.51
MRSI-NR-1-3w-25c NM	25	Mid	No	265	23.19	-6.52	-6.54	1.03	29.49
MRSI-NR-2-3w-25c NM	25	Mid	No	146	23.30	-6.48	-6.5	1.03	29.55
MRSI-NR-1-5w-25c NM	25	Mid	No	238	23.31	-6.45	-6.44	1.03	29.50
MRSI-NR-1-7w-25c NM	25	Mid	No	126	23.32	-6.54	-6.58	1.03	29.65
MRSI-NR-2-7w-25c NM	25	Mid	No	241	23.18	-6.46	-6.44	1.03	29.38
MRSI-NR-2-1w-5c NM	5	Mid	No	3	22.56	-6.46	-6.49	1.03	28.82
MRSI-NR-2-3w-5c NM	5	Mid	No	6	23.01	-6.45	-6.5	1.03	29.27
MRSI-NR-2-5w-5c NM	5	Mid	No	1	22.33	-6.54	-6.47	1.03	28.58
MRSI-NR-1-7w-5c NM	5	Mid	No	5	22.45	-6.55	-6.56	1.03	28.78
MRSI-NR-2-7w-5c NM	5	Mid	No	3	22.54	-6.64	-6.64	1.03	28.95
MRSI-NR-2-1w-15c NM	15	Mid	No	180	23.21	-6.54	-6.55	1.03	29.52
MRSI-NR-1-3w-15c NM	15	Mid	No	135	23.12	-6.53	-6.53	1.03	29.41
MRSI-NR-1-5w-15c NM	15	Mid	No	143	23.27	-6.39	-6.4	1.03	29.42
MRSI-NR-2-5w-15c NM	15	Mid	No	174	23.10	-6.51	-6.51	1.03	29.37
MRSI-NR-1-7w-15c NM	15	Mid	No	172	23.15	-6.56	-6.57	1.03	29.48
MRSI-NR-2-7w-15c NM	15	Mid	No	97	23.17	-6.47	-5.72	1.03	28.65
MRSI-NR-2-1w-25c NM	25	Mid	No	246	23.53	-6.49	-6.48	1.03	29.76
MRSI-NR-1-3w-25c NM	25	Mid	No	297	23.53	-6.52	-6.54	1.03	29.82
MRSI-NR-2-3w-25c NM	25	Mid	No	314	23.43	-6.48	-6.5	1.03	29.68
MRSI-NR-1-5w-25c NM	25	Mid	No	212	23.58	-6.45	-6.44	1.03	29.77
MRSI-NR-1-7w-25c NM	25	Mid	No	289	23.52	-6.54	-6.58	1.03	29.85
MRSI-NR-2-7w-25c NM	25	Mid	No	301	23.25	-6.46	-6.44	1.03	29.45
MRSI-NR 25 1-NM	25	Mid	No	329	23.52	-6.45	-6.47	1.03	29.74
MRSI-NR 50MM 1-NM	50	Mid	No	1432	23.88	-6.21	-6.2	1.03	29.81
MRSI-NR 50MM 2-NM	50	Mid	No	1398	24.02	-6.14	-6.1	1.03	29.85
MRSI-NR 25 OB 1-NM	25	Mid	No	328	23.29	-6.74	-6.75	1.03	29.80

MRSI-NR 25 OB 2-NM	25	Mid	No	391	23.37	-6.69	-6.71	1.03	29.83
MRSI-NR-1-5c-LLM	5	Mid	No	3	22.76	-6.46	-6.46	1.03	28.98
MRSI-NR-2-5c-LLM	5	Mid	No	3	22.66	-6.47	-6.46	1.03	28.88
MRSI-NR-1-7c-LLM	7	Mid	No	7	22.46	-6.42	-6.40	1.03	28.63
MRSI-NR-2-7c-LLM	7	Mid	No	6	22.48	-6.41	-6.42	1.03	28.67
MRSI-NR-1-10c-LLM	10	Mid	No	98	22.86	-6.46	-6.45	1.03	29.08
MRSI-NR-2-10c-LLM	10	Mid	No	111	22.56	-6.42	-6.42	1.03	28.74
MRSI-NR-1-15c-LLM	15	Mid	No	110	23.32	-6.49	-6.49	1.03	29.56
MRSI-NR-2-15c-LLM	15	Mid	No	90	23.38	-6.47	-6.47	1.03	29.60
MRSI-NR-1-25c-LLM	25	Mid	No	260	23.43	-6.47	-6.51	1.03	29.70
MRSI-NR-2-25c-LLM	25	Mid	No	300	23.43	-6.48	-6.54	1.03	29.72
MRSI-NR-1-5C-PSA	5	Mid	No	4	22.29	-6.49	-6.46	1.03	28.53
MRSI-NR-2-5C-PSA	5	Mid	No	43	22.30	-6.47	-6.44	1.03	28.52
MRSI-NR-1-15C-PSA	15	Mid	No	86	22.91	-6.45	-6.41	1.03	29.08
MRSI-NR-2-15C-PSA	15	Mid	No	94	22.93	-6.43	-6.40	1.03	29.09
MRSI-NR-1-25C-PSA	25	Mid	No	140	23.02	-6.47	-6.43	1.03	29.21
MRSI-NR-2-25C-PSA	25	Mid	No	97	23.09	-6.49	-6.45	1.03	29.30
MRSI-NR 5mmolal 5CA PSA2	5	Mid	Yes	3	22.21	-6.46	-6.43	1.03	28.41
MRSI-NR 5mmolal 15CA PSA2	5	Mid	Yes	2	22.32	-6.45	-6.41	1.03	28.51
MRSI-NR 5mmolal 25CA PSA2	5	Mid	Yes	3	22.37	-6.47	-6.46	1.03	28.60
MRSI-NR 15mmolal 5CA PSA2	15	Mid	Yes	190	23.11	-6.49	-6.46	1.03	29.33
MRSI-NR 15mmolal 15CA PSA2	15	Mid	Yes	230	22.96	-6.47	-6.49	1.03	29.21
MRSI-NR 15mmolal 25CA PSA2	15	Mid	Yes	215	22.89	-6.48	-6.47	1.03	29.13
MRSI-NR 25mmolal 5CA PSA2	25	Mid	Yes	218	23.38	-6.46	-6.51	1.03	29.64
MRSI-NR 25mmolal 15CA PSA2	25	Mid	Yes	245	23.42	-6.5	-6.48	1.03	29.65
MRSI-NR 25mmolal 25CA PSA2	25	Mid	Yes	350	23.49	-6.46	-6.43	1.03	29.67
MRSI-NR 15mmolal 38µM PSA 1	15	Mid	Yes	300	23.23	-6.46	-6.41	1.03	29.39
MRSI-NR 15mmolal 38µM PSA 2	15	Mid	Yes	275	23.12	-6.45	-6.43	1.03	29.31
MRSI-NR 25mmolal 38µM PSA 1	25	Mid	Yes	433	22.92	-6.43	-6.44	1.03	29.12
MRSI-NR 25mmolal 38µM PSA 2	25	Mid	Yes	350	22.87	-6.46	-6.49	1.03	29.12
MRSI-NR 5mm 5CA	5	Mid	Yes	3	22.54	-6.44	-6.46	1.03	28.77
MRSI-NR 5mm 15CA	5	Mid	Yes	3	22.57	-6.44	-6.43	1.03	28.77
MRSI-NR 5mm 25CA	5	Mid	Yes	2	22.76	-6.46	-6.48	1.03	29.01
MRSI-NR 25mm 5CA	25	Mid	Yes	204	23.60	-6.43	-6.41	1.03	29.76
MRSI-NR 25mm 15CA	25	Mid	Yes	251	23.40	-6.44	-6.43	1.03	29.59
NR 7d 10pH 5 -1	5	High	No	480	20.04	-6.45	-6.42	1.03	26.28

NR 7d 10pH 5 -2	5	High	No	420	19.98	-6.43	-6.41	1.03	26.21
NR 50d 10pH 5- 1	5	High	No	440	19.99	-6.41	-6.39	1.03	26.20
NR 50d 10pH 5- 2	5	High	No	450	19.95	-6.41	-6.37	1.03	26.14
NR 7d 10pH 25- 1	25	High	No	1900	18.76	-6.40	-6.38	1.03	24.99
NR 7d 10pH 25- 2	25	High	No	1800	18.77	-6.40	-6.38	1.03	25.00
NR 7d 10pH 25- 3	25	High	No	1600	18.76	-6.40	-6.4	1.03	25.01
NR 7d 10pH 25- 4	25	High	No	1300	18.74	-6.41	-6.43	1.03	25.02
NR 50d 10pH 50 25- 3	25	High	No	1500	18.94	-6.43	-6.44	1.03	25.22
NR 50d 10pH 50 25- 4	25	High	No	1900	18.94	-6.40	-6.39	1.03	25.17
NR 50d 10pH 50 25- 5	25	High	No	1800	19.01	-6.39	-6.36	1.03	25.21
NR 50d 10pH 50 25- 6	25	High	No	2000	19.01	-6.40	-6.35	1.03	25.20

Table 2.5. Experimental Data of Carbon for Calcite

Sample ID	**Ca^{2+} and DIC conc.**	**pH**	**$CaCO_3$ (mg)**	$\delta^{13}C_{CaCO_3}$	$\delta^{13}C_{NaHCO_3}$ or Na_2CO_3	**DIC_{ini} (mmolal)**	$\delta^{13}C_{DIC_{ini}}$	**DIC_{fin} (mmolal)**	$\delta^{13}C_{DIC_{fin}}$	$\alpha_{CaCO_3\text{-}DIC}$	$1000\ln^{13}\alpha_{(CaCO3\text{-}DIC)}$
MRSI-NR-2-1w-5c NM	5	Mid	2	-24.01	-25.81	5.1	N/A	4.58	N/A	N/A	N/A
MRSI-NR-2-3w-5c NM	5	Mid	2	-24.32	-25.81	4.7	N/A	4.23	N/A	N/A	N/A
MRSI-NR-1-7w-5c NM	5	Mid	2	-23.90	-25.81	4.6	N/A	4.09	N/A	N/A	N/A
MRSI-NR-2-7w-5c NM	5	Mid	3	-24.25	-25.81	5	N/A	4.45	N/A	N/A	N/A
MRSI-NR-2-1w-15c NM	15	Mid	96	-22.99	-25.81	14.7	N/A	11.33	N/A	N/A	N/A
MRSI-NR-1-3w-15c NM	15	Mid	91	-24.31	-25.81	14.8	N/A	10.95	N/A	N/A	N/A
MRSI-NR-1-5w-15c NM	15	Mid	94	-22.45	-25.81	14.6	N/A	11.53	N/A	N/A	N/A
MRSI-NR-2-5w-15c NM	15	Mid	81	-22.83	-25.81	15.1	N/A	11.33	N/A	N/A	N/A
MRSI-NR-1-7w-15c NM	15	Mid	74	-22.86	-25.81	15	N/A	11.40	N/A	N/A	N/A
MRSI-NR-2-7w-15c NM	15	Mid	79	-22.13	-25.81	14.9	N/A	11.32	N/A	N/A	N/A
MRSI-NR-2-1w-25c NM	25	Mid	180	-22.51	-25.81	24.2	N/A	13.07	N/A	N/A	N/A
MRSI-NR-1-3w-25c NM	25	Mid	210	-23.05	-25.81	24.9	N/A	13.20	N/A	N/A	N/A

MRSI-NR-2-3w-25c NM	25	Mid	230	-22.31	-25.81	24.7	N/A	14.57	N/A	N/A	N/A
MRSI-NR-1-5w-25c NM	25	Mid	246	-23.24	-25.81	24.8	N/A	14.19	N/A	N/A	N/A
MRSI-NR-1-7w-25c NM	25	Mid	312	-22.49	-25.81	24.9	N/A	13.94	N/A	N/A	N/A
MRSI-NR-2-7w-25c NM	25	Mid	201	-22.61	-25.81	24.6	N/A	13.28	N/A	N/A	N/A
MRSI-NR-2-1w-5c NM	5	Mid	2	-24.49	-25.81	5.1	N/A	4.58	N/A	N/A	N/A
MRSI-NR-2-3w-5c NM	5	Mid	2	-23.43	-25.81	4.7	N/A	4.23	N/A	N/A	N/A
MRSI-NR-1-7w-5c NM	5	Mid	4	-24.15	-25.81	4.6	N/A	4.09	N/A	N/A	N/A
MRSI-NR-2-7w-5c NM	5	Mid	8	-24.35	-25.81	5	N/A	4.45	N/A	N/A	N/A
MRSI-NR-2-1w-15c NM	15	Mid	187	-23.11	-25.81	14.7	N/A	11.33	N/A	N/A	N/A
MRSI-NR-1-3w-15c NM	15	Mid	164	-22.53	-25.81	14.8	N/A	10.95	N/A	N/A	N/A
MRSI-NR-1-5w-15c NM	15	Mid	182	-24.05	-25.81	14.6	N/A	11.53	N/A	N/A	N/A
MRSI-NR-2-5w-15c NM	15	Mid	152	-23.54	-25.81	15.1	N/A	11.33	N/A	N/A	N/A
MRSI-NR-1-7w-15c NM	15	Mid	125	-23.20	-25.81	15	N/A	11.40	N/A	N/A	N/A
MRSI-NR-2-7w-15c NM	15	Mid	123	-23.21	-25.81	14.9	N/A	11.32	N/A	N/A	N/A
MRSI-NR-2-1w-25c NM	25	Mid	234	-22.85	-25.81	24.2	N/A	13.07	N/A	N/A	N/A
MRSI-NR-1-3w-25c NM	25	Mid	265	-22.98	-25.81	24.9	N/A	13.20	N/A	N/A	N/A
MRSI-NR-2-3w-25c NM	25	Mid	146	-22.44	-25.81	24.7	N/A	14.57	N/A	N/A	N/A
MRSI-NR-1-5w-25c NM	25	Mid	238	-22.58	-25.81	24.8	N/A	14.19	N/A	N/A	N/A
MRSI-NR-1-7w-25c NM	25	Mid	126	-22.74	-25.81	24.9	N/A	13.94	N/A	N/A	N/A
MRSI-NR-2-7w-25c NM	25	Mid	241	-22.68	-25.81	24.6	N/A	13.28	N/A	N/A	N/A
MRSI-NR-2-1w-5c NM	5	Mid	3	-24.36	-25.81	5.1	N/A	4.58	N/A	N/A	N/A
MRSI-NR-2-3w-5c NM	5	Mid	6	-23.10	-25.81	4.7	N/A	4.23	N/A	N/A	N/A
MRSI-NR-2-5w-5c NM	5	Mid	1	-24.00	-25.81	4.6	N/A	4.23	N/A	N/A	N/A
MRSI-NR-1-7w-5c NM	5	Mid	5	-24.27	-25.81	5	N/A	4.09	N/A	N/A	N/A
MRSI-NR-2-7w-5c NM	5	Mid	3	-24.30	-25.81	4.7	N/A	4.45	N/A	N/A	N/A
MRSI-NR-2-1w-15c NM	15	Mid	180	-22.96	-25.81	14.8	N/A	11.41	N/A	N/A	N/A
MRSI-NR-1-3w-15c NM	15	Mid	135	-23.06	-25.81	14.6	N/A	10.80	N/A	N/A	N/A
MRSI-NR-1-5w-15c NM	15	Mid	143	-22.56	-25.81	15.1	N/A	11.93	N/A	N/A	N/A
MRSI-NR-2-5w-15c NM	15	Mid	174	-23.05	-25.81	14.9	N/A	11.18	N/A	N/A	N/A

MRSI-NR-1-7w-15c NM	15	Mid	172	-22.99	-25.81	15	N/A	11.40	N/A	N/A	N/A
MRSI-NR-2-7w-15c NM	15	Mid	97	-23.00	-25.81	14.9	N/A	11.32	N/A	N/A	N/A
MRSI-NR-2-1w-25c NM	25	Mid	246	-22.43	-25.81	24.2	N/A	13.07	N/A	N/A	N/A
MRSI-NR-1-3w-25c NM	25	Mid	297	-22.4 6	-25.81	24.9	N/A	13.20	N/A	N/A	N/A
MRSI-NR-2-3w-25c NM	25	Mid	314	-22.73	-25.81	24.7	N/A	14.57	N/A	N/A	N/A
MRSI-NR-1-5w-25c NM	25	Mid	212	-22.37	-25.81	24.8	N/A	14.19	N/A	N/A	N/A
MRSI-NR-1-7w-25c NM	25	Mid	289	-22.34	-25.81	24.9	N/A	13.94	N/A	N/A	N/A
MRSI-NR-2-7w-25c NM	25	Mid	301	-22.76	-25.81	24.6	N/A	13.28	N/A	N/A	N/A
MRSI-NR 25 1 NM	25	Mid	329	-2.99	-6.97	24.7	-6.94	13.34	-5.500	1.0040	3.97
MRSI-NR 50MM NM	50	Mid	1432	-3.59	-6.97	49.7	-6.91	N/A	-7.300	1.0033	3.34
MRSI-NR 50MM 2 NM	50	Mid	1398	-3.03	-6.97	49.9	-6.89	N/A	-7.100	1.0039	3.88
MRSI-NR 25 OB 1 NM	25	Mid	328	-3.21	-6.97	25.1	-6.95	14.06	-5.500	1.0038	3.76
MRSI-NR 25 OB 2 NM	25	Mid	391	-3.40	-6.97	25.2	-6.86	13.36	-5.500	1.0035	3.48
MRSI-NR-1-5c-LLM	5	Mid	3	-24.67	-25.81	4.7	-25.86	4.12	-25.78	1.0012	1.22
MRSI-NR-2-5c-LLM	5	Mid	3	-24.61	-25.81	4.9	-25.71	4.26	-25.89	1.0011	1.13
MRSI-NR-1-7c-LLM	7	Mid	7	-24.58	-25.81	6.9	-25.89	5.30	-25.83	1.0013	1.34
MRSI-NR-2-7c-LLM	7	Mid	6	-24.2	-25.81	6.9	-25.79	5.37	-25.34	1.0016	1.63
MRSI-NR-1-10c-LLM	10	Mid	98	-24.11	-25.81	9.8	-25.77	7.20	-25.48	1.0017	1.70
MRSI-NR-2-10c-LLM	10	Mid	111	-24.05	-25.81	9.6	-25.83	6.98	-25.79	1.0018	1.83
MRSI-NR-1-15c-LLM	15	Mid	110	-23.71	-25.81	14.7	-25.78	10.09	-25.76	1.0021	2.12
MRSI-NR-2-15c-LLM	15	Mid	90	-23.12	-25.81	14.9	-25.8	9.66	-25.92	1.0028	2.75
MRSI-NR-1-25c-LLM	25	Mid	260	-23.62	-25.81	24.7	-25.81	13.94	-26.95	1.0022	2.24
MRSI-NR-2-25c-LLM	25	Mid	300	-23.68	-25.81	24.8	-25.84	13.58	-26.77	1.0022	2.22
MRSI-NR-1-5C-PSA	5	Mid	4	-25.21	-25.81	4.8	-25.82	4.26	-25.67	1.0006	0.63
MRSI-NR-2-5C-PSA	5	Mid	43	-25.19	-25.81	5	-25.79	4.34	-25.59	1.0006	0.61
MRSI-NR-1-15C-PSA	15	Mid	86	-23.10	-25.81	14.6	-25.82	10.02	-25.49	1.0028	2.79
MRSI-NR-2-15C-PSA	15	Mid	94	-23.22	-25.81	14.6	-25.79	9.47	-25.46	1.0026	2.63
MRSI-NR-1-25C-PSA	25	Mid	140	-23.62	-25.81	24.6	-25.8	14.45	-25.36	1.0022	2.24
MRSI-NR-2-25C-PSA	25	Mid	97	-23.13	-25.81	24.8	-25.77	14.30	-25.30	1.0027	2.71
MRSI-NR 5mmolal 5CA PSA2	5	Mid	3	-5.26	-6.97	4.7	-6.98	4.16	-6.07	1.0017	1.73
MRSI-NR 5mmolal 15CA PSA2	5	Mid	2	-5.33	-6.97	4.8	-6.95	4.16	-6.07	1.0016	1.63
MRSI-NR 5mmolal 25CA PSA2	5	Mid	3	-5.05	-6.97	4.8	-6.89	4.07	-6.19	1.0019	1.85
MRSI-NR 15mmolal 5CA PSA2	15	Mid	190	-3.80	-6.97	14.6	-6.93	9.86	-6.23	1.0031	3.14
MRSI-NR 15mmolal 15CA PSA2	15	Mid	230	-3.79	-6.97	14.8	-6.97	9.85	-6.02	1.0032	3.20

MRSI-NR 15mmolal 25CA PSA2	15	Mid	215	-3.67	-6.97	15.1	-6.95	10.20	-6.28	1.0033	3.30
MRSI-NR 25mmolal 5CA PSA2	25	Mid	218	-3.28	-6.97	24.9	-6.95	13.63	-6.42	1.0037	3.69
MRSI-NR 25mmolal 15CA PSA2	25	Mid	245	-3.34	-6.97	25.2	-6.94	14.51	-6.76	1.0036	3.62
MRSI-NR 25mmolal 25CA PSA2	25	Mid	350	-3.17	-6.97	25.4	-6.97	13.57	-6.42	1.0038	3.82
MRSI-NR 15mmolal 38µM PSA 1	15	Mid	300	-3.90	-6.97	14.8	-6.89	11.25	-5.88	1.0030	3.01
MRSI-NR 15mmolal 38µM PSA 2	15	Mid	275	-3.89	-6.97	15.2	-6.92	12.16	-5.52	1.0030	3.04
MRSI-NR 25mmolal 38µM PSA 1	25	Mid	433	-3.18	-6.97	25.4	-6.94	14.73	-5.66	1.0038	3.78
MRSI-NR 25mmolal 38µM PSA 2	25	Mid	350	-3.26	-6.97	25.6	-6.97	13.82	-5.74	1.0037	3.73
MRSI-NR 5mm 5CA	5	Mid	3	-5.00	-6.97	5.5	-6.91	5.01	-6.22	1.0019	1.92
MRSI-NR 5mm 15CA	5	Mid	3	-4.99	-6.97	5.2	-6.94	4.63	-6.28	1.0020	1.96
MRSI-NR 5mm 25CA	5	Mid	2	-5.14	-6.97	4.9	-6.98	4.26	-6.39	1.0019	1.85
MRSI-NR 25mm 5CA	25	Mid	204	-3.12	-6.97	25.3	-6.95	13.41	-6.27	1.0039	3.85
MRSI-NR 25mm 15CA	25	Mid	251	-3.04	-6.97	25.4	-6.99	13.72	-6.76	1.0040	3.97
NR 7d 10pH 5 -1	5	High	480	-1.80	-1.91	4.96	-2.05	0.39	-3.44	1.0002	0.25
NR 7d 10pH 5 -2	5	High	420	-1.75	-1.91	4.65	-1.96	0.39	-3.46	1.0002	0.21
NR 50d 10pH 5- 1	5	High	440	-1.72	-1.91	4.68	-1.95	0.38	-3.48	1.0002	0.23
NR 50d 10pH 5- 2	5	High	450	-1.72	-1.91	4.85	-1.94	0.39	-3.34	1.0002	0.22
NR 7d 10pH 25- 1	25	High	1900	-1.75	-1.91	24.34	-1.96	0.71	-3.81	1.0002	0.22
NR 7d 10pH 25- 2	25	High	1800	-1.73	-1.91	24.38	-1.94	0.60	-3.81	1.0002	0.21
NR 7d 10pH 25- 3	25	High	1600	-1.72	-1.91	23.43	-1.93	0.70	-3.85	1.0002	0.21
NR 7d 10pH 25- 4	25	High	1300	-1.73	-1.91	23.04	-1.93	0.58	-3.84	1.0002	0.20
NR 50d 10pH 50 25- 3	25	High	1500	-1.78	-1.91	24.87	-1.97	0.70	-3.82	1.0002	0.19
NR 50d 10pH 50 25- 4	25	High	1900	-1.79	-1.91	25.13	-1.92	0.70	-3.82	1.0001	0.13
NR 50d 10pH 50 25- 5	25	High	1800	-1.75	-1.91	25.49	-1.91	0.76	-3.87	1.0002	0.16
NR 50d 10pH 50 25- 6	25	High	2000	-1.73	-1.91	25.37	-1.96	0.76	-3.85	1.0002	0.23

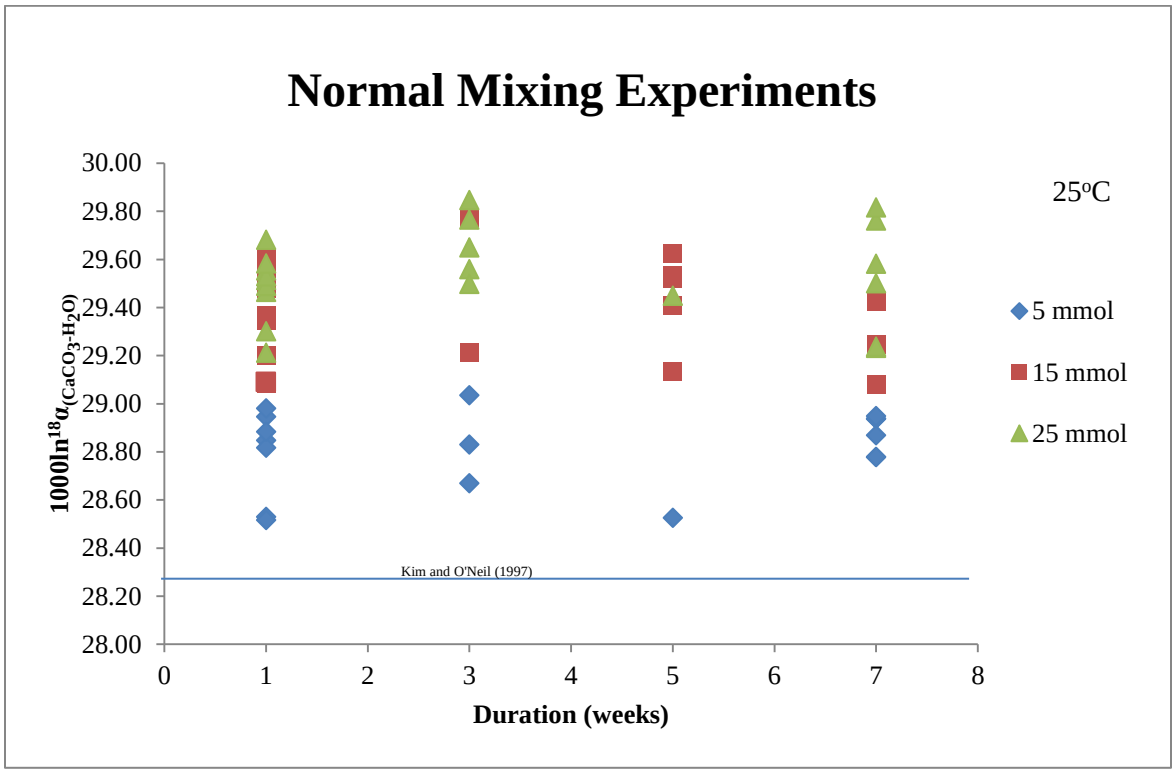

Figure 2.4. A comparison of the $1000\ln^{18}\alpha_{(CaCO_3\text{-}H_2O)}$ versus the duration of time which elapsed after the addition of $CaCl_2$. The overall similarity in the oxygen isotope fractionation factors between $CaCO_3$ and water of each concentration over the allotted time suggests that the carbonates completely precipitated within a week and did not continue to precipitate afterwards. The fast precipitation signifies that kinetic effects occurred within the system.

Table 2.6. A Summary of the analyzed catalyzed data compared to some of the uncatalyzed data.

Experiment Type	Precipitation Method	Sample I.D.	$1000\ln^{18}\alpha_{(CaCO3\text{-}H2O)}$	$1000\ln^{13}\alpha_{(CaCO3\text{-}DIC)}$
CA Experiments	Partial Solid Addition	MRSI-NR 5mmolal 5CA SA2	28.41	0.81
		MRSI-NR 5mmolal 15CA SA2	28.51	0.75
		MRSI-NR 5mmolal 25CA SA2	28.60	1.15
		MRSI-NR 15mmolal 5CA SA2	29.33	2.44
		MRSI-NR 15mmolal 15CA SA2	29.21	2.24
		MRSI-NR 15mmolal 25CA SA2	29.13	2.62
		MRSI-NR 15mmolal 38µM SA 1	29.66	1.99
		MRSI-NR 15mmolal 38µM SA 2	29.87	1.63
		MRSI-NR 25mmolal 5CA SA2	29.64	3.16
		MRSI-NR 25mmolal 15CA SA2	29.65	3.44
		MRSI-NR 25mmolal 25CA SA2	29.67	3.27
		MRSI-NR 25mmolal 38µM SA 1	29.28	2.50
		MRSI-NR 25mmolal 38µM SA 2	29.18	2.49
	Normal Mixing	MRSI-NR 5mm 5CA	28.77	1.23
		MRSI-NR 5mm 15CA	28.77	1.29
		MRSI-NR 5mm 25CA	29.01	1.25
		MRSI-NR 25mm 5CA	29.76	3.17
		MRSI-NR 25mm 15CA	29.59	3.73
Uncatalyzed Experiments	Normal	MRSI-NR-5mmolal	28.82	1.48
		MRSI-NR-5mmolal	28.78	1.58
		MRSI-NR-15mmolal	29.52	2.92
		MRSI-NR-15mmolal	29.41	2.82
		MRSI-NR-25mmolal	29.85	3.56
		MRSI-NR-25mmolal	29.45	3.13
	Partial Solid Addition	MRSI-NR 5mmolal SA1	28.53	0.88
		MRSI-NR 5mmolal SA2	28.52	0.91
		MRSI-NR 15mmolal SA1	29.08	2.87
		MRSI-NR 15mmolal SA2	29.09	2.73
		MRSI-NR 25mmolal SA1	29.04	2.20
		MRSI-NR 25mmolal SA2	29.30	2.65
	Liquid/Liquid	MRSI-NR 5mmolal LL1	28.98	1.66
		MRSI-NR 5mmolal LL2	28.19	1.15
		MRSI-NR 15mmolal LL1	29.56	3.55
		MRSI-NR 15mmolal LL2	29.20	2.90
		MRSI-NR 25mmolal LL1	29.53	4.56
		MRSI-NR 25mmolal LL2	29.58	3.76

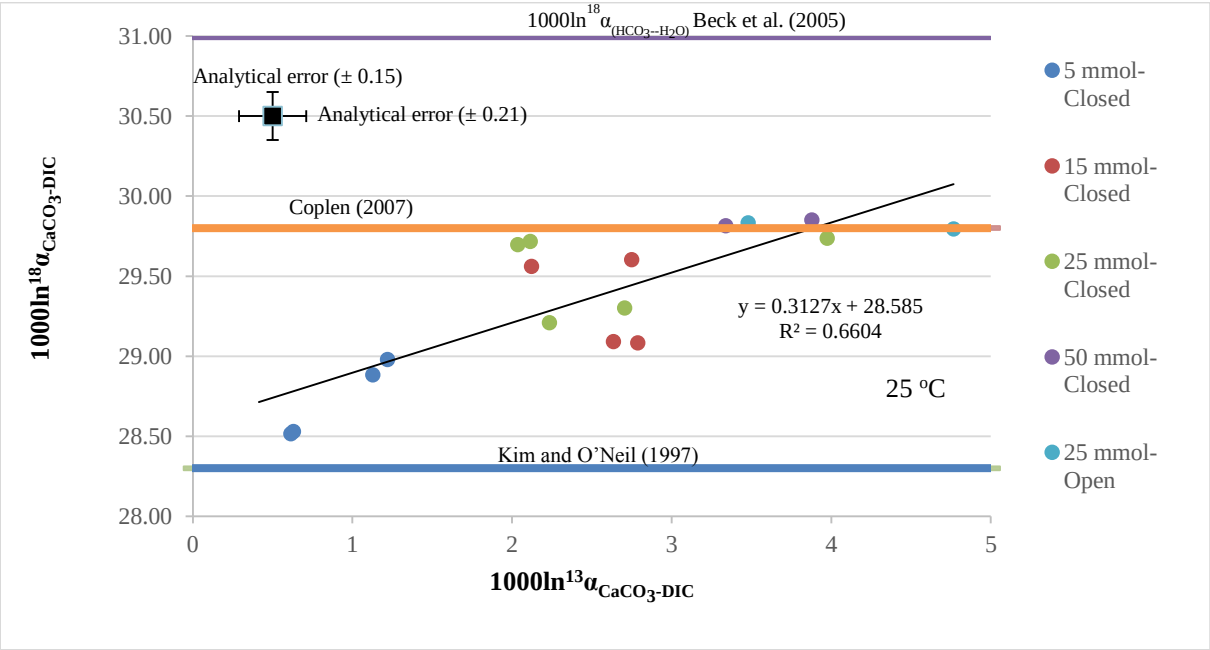

Figure 2.5. A comparison of the oxygen and carbon isotope fractionation factors of all of samples precipitated in this study at different concentrations. Some samples exceed 29.8 ‰, however this is within analytical error.

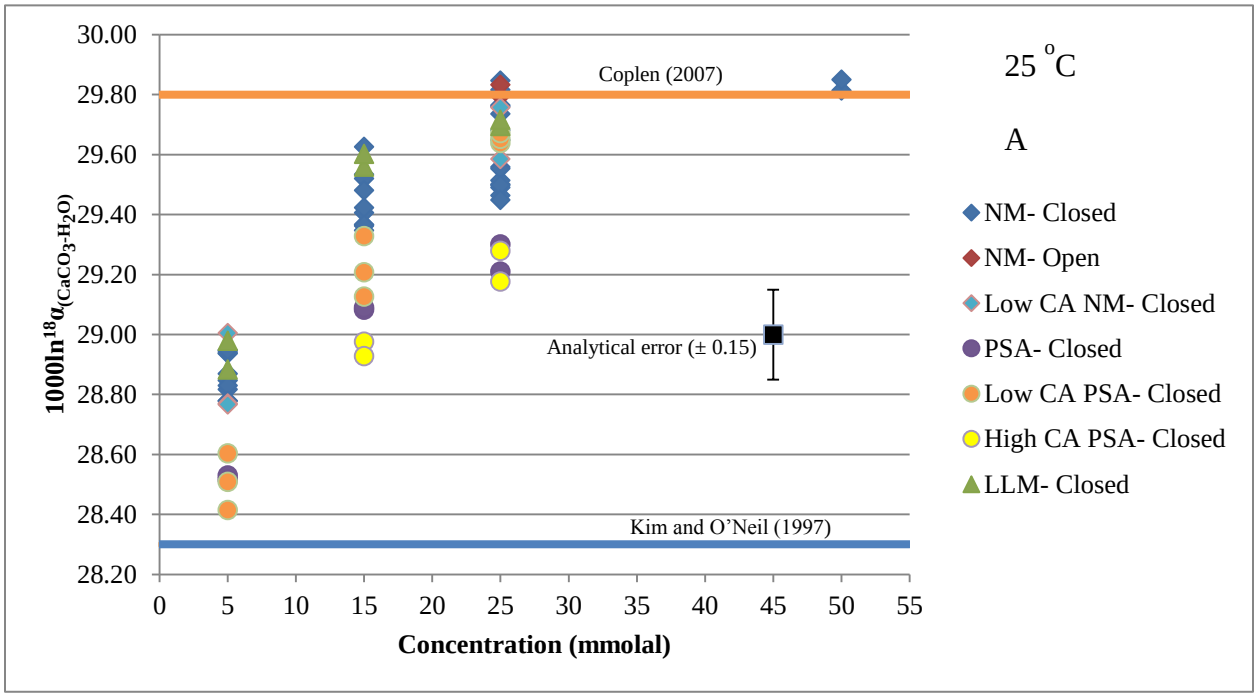

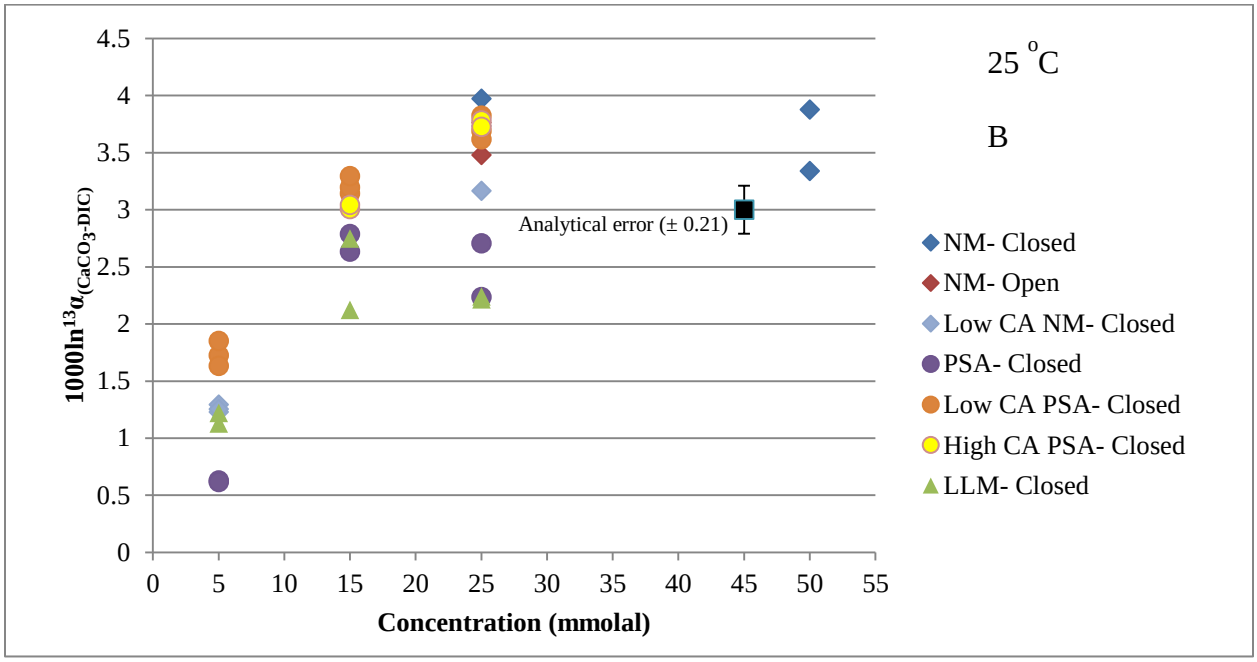

Figure 2.6. A comparison of the isotopic fractionation factors of oxygen (A) and carbon (B) with concentration. Both of these figures illustrate that there is an upper barrier in which the samples cannot penetrate in the system.

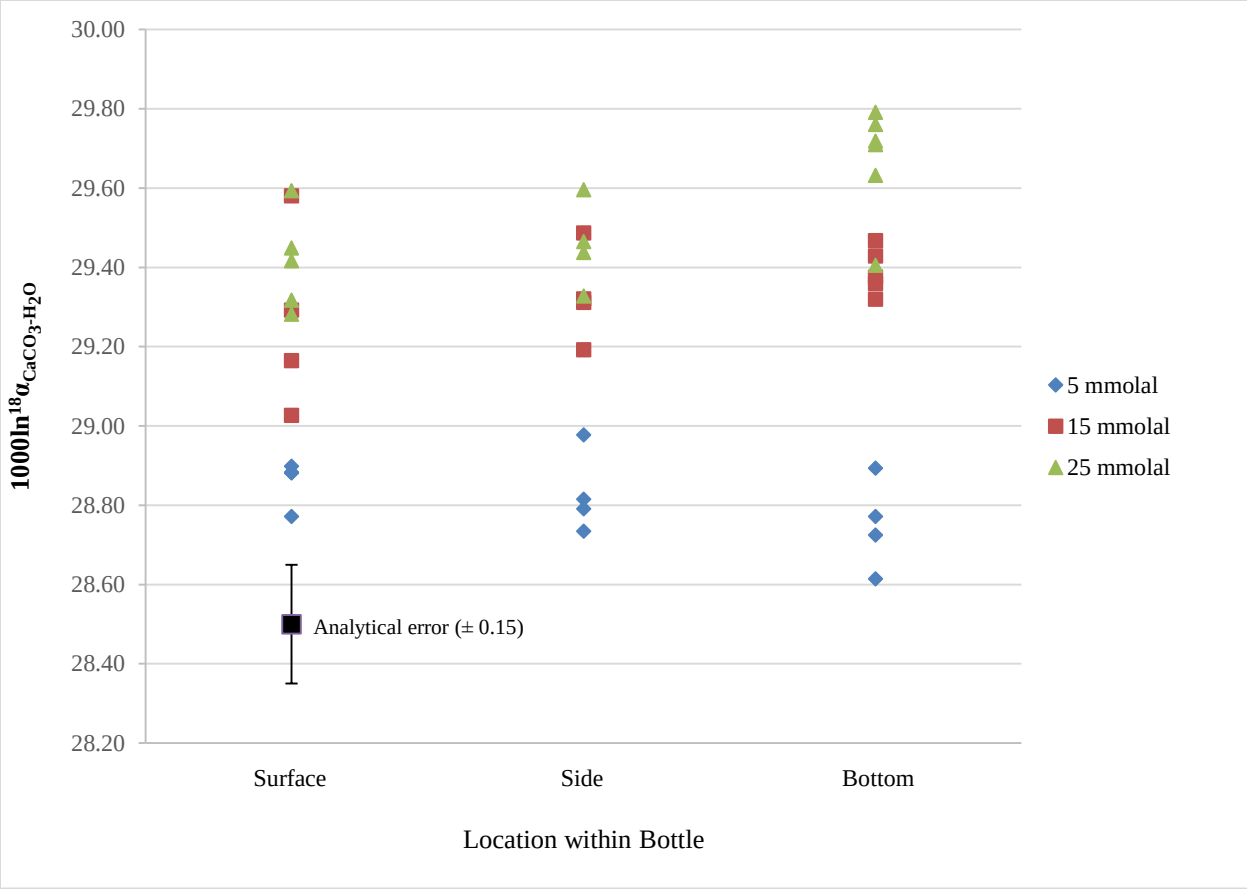

Figure 2.7. A comparison of the oxygen and carbon isotope fractionation factor of the calcite samples precipitated at the surface, side and bottom of the bottle in which they were synthesized. The overall similarity in isotopic fractionation factor is strictly due to $CO_{2(aq)}$ production caused by Type II CPM. The variation present within the data at higher fraction values is most likely due to analytical error.

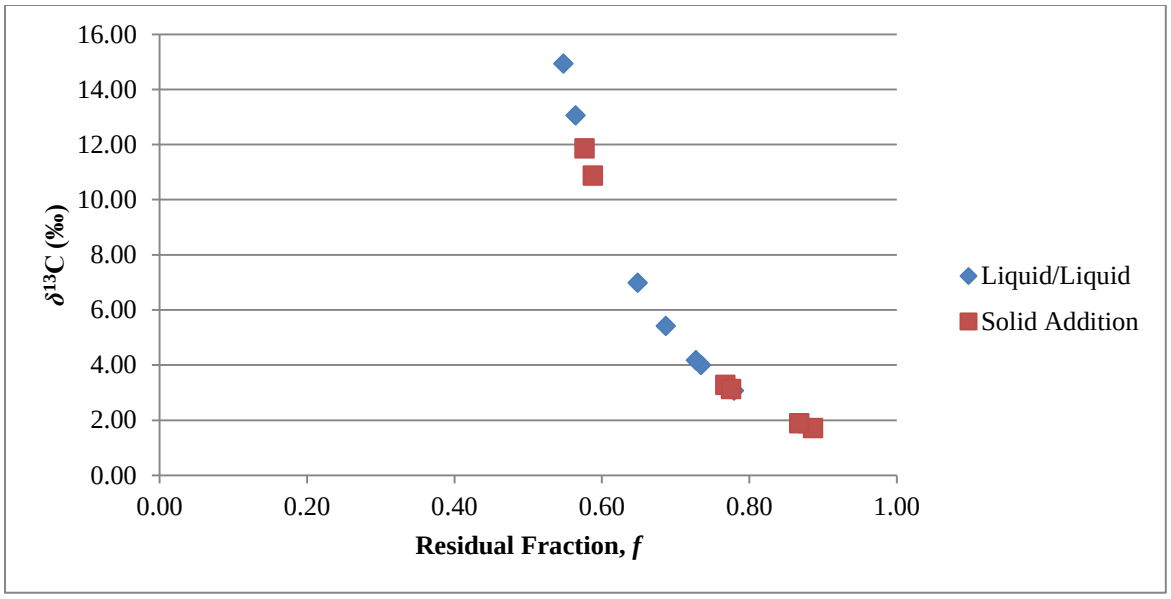

Figure 2.8. Rayleigh distillation curve for the PSA and LLM samples. All samples precipitated in these experiments followed similar curve. The figure shows an exponential increase in carbon-13 with increasing consumption of the DIC reservoir.

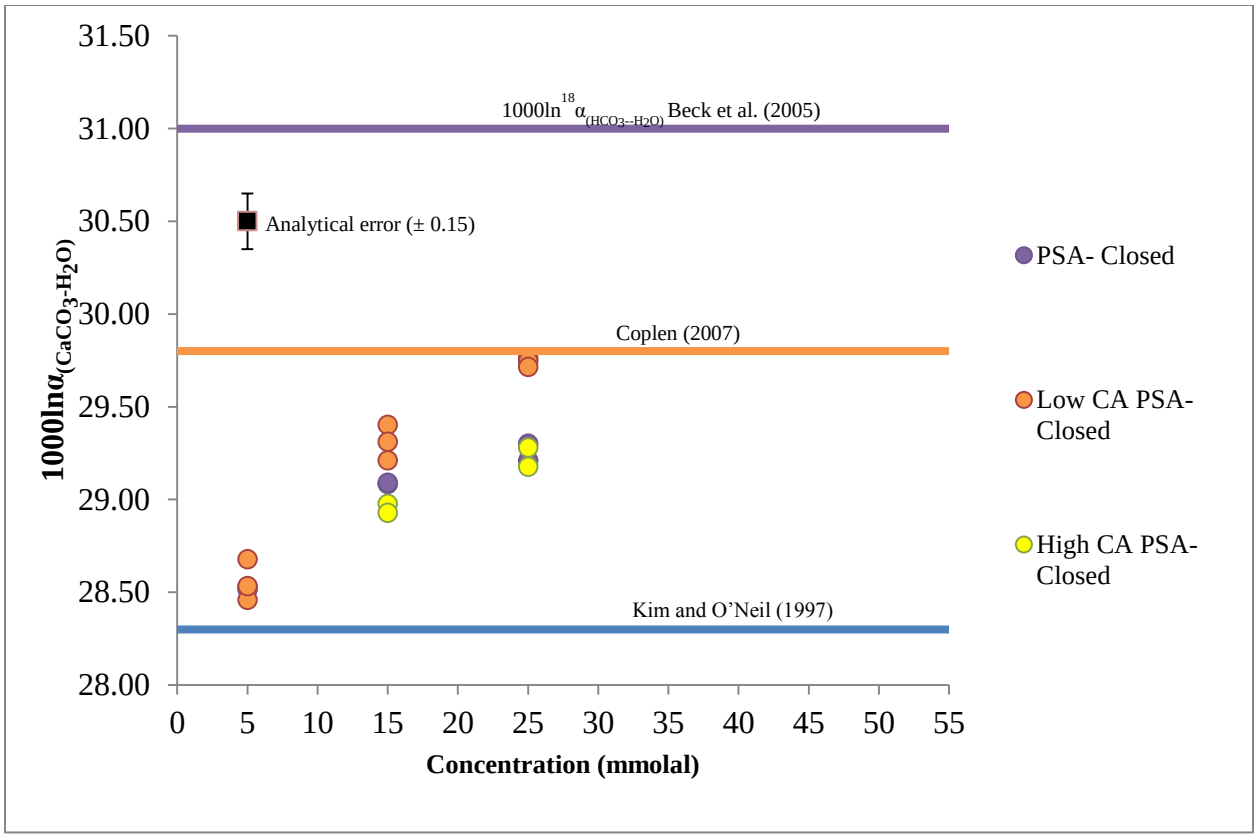

Figure 2.9. A comparison of the data from the CA experiments with all of data from the mid-pH, uncatalyzed PSA experiments. All of the CA experiments presented here precipitated using the

PSA technique. The carbon and oxygen fractionation factor value of the experiments catalyzed with relatively low concentrations of CA are all comparable to those of the PSA experiments, which had the slowest precipitation rate. This signifies that precipitation rate always outpaced the catalyzing effect of the enzyme. The samples precipitated in the presence of 38µM of CA (double that used by Watkins et al (2013)) have lower carbon and oxygen isotopic fractionation factors and are closer to the equilibrium values proposed by Kim and O'Neil (1997) and Romanek et al. (1992). These experiments were not conducted at 5 mmolal since the acidifying effect of CA prevented carbonate growth.

Table 2.7: Percent composition of DIC consumed in mid-pH experiments

Sample Concentration	**% of DIC Precipitated**
5 mmolal	11-12 %
15 mmolal	32-33 %
25 mmolal	44-45 %

Table 2.8: Percent composition of DIC consumed in high pH experiments

Sample Concentration	**% of DIC Precipitated**
5 mmolal	91-92 %
15 mmolal	94-95 %
25 mmolal	96-98 %

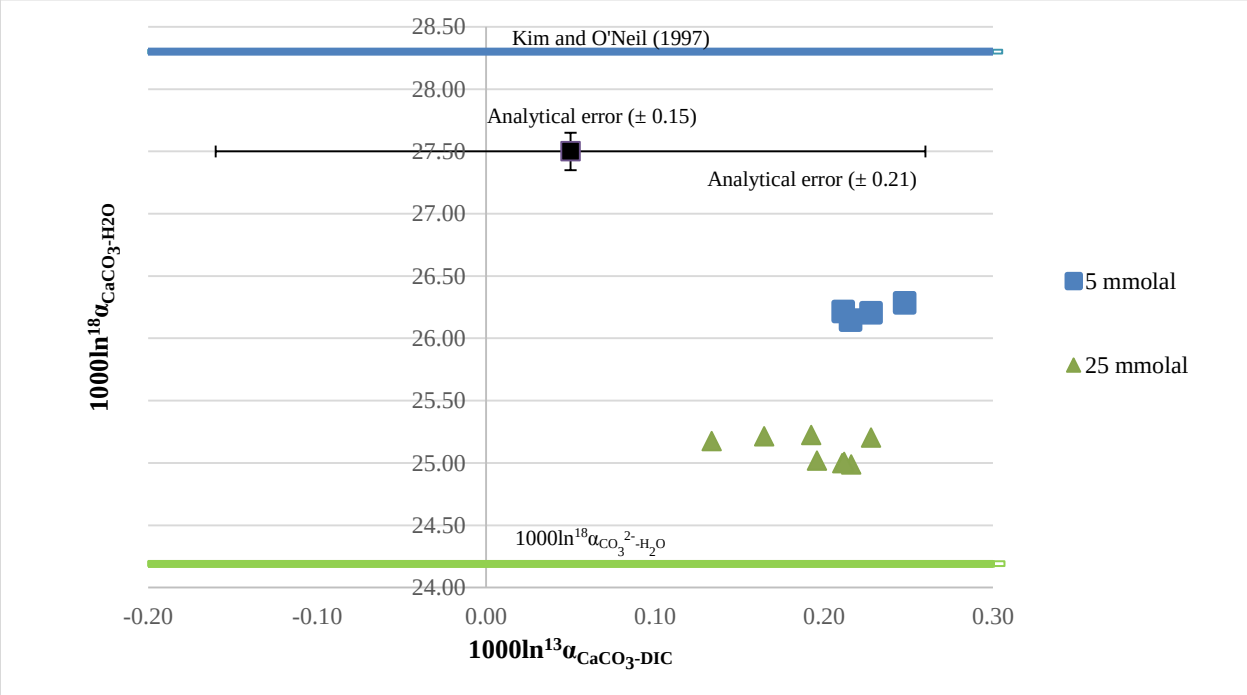

Figure 2.10: A comparison of the oxygen and carbon isotope fractionation factors of the high pH samples precipitated in this study at different concentrations.

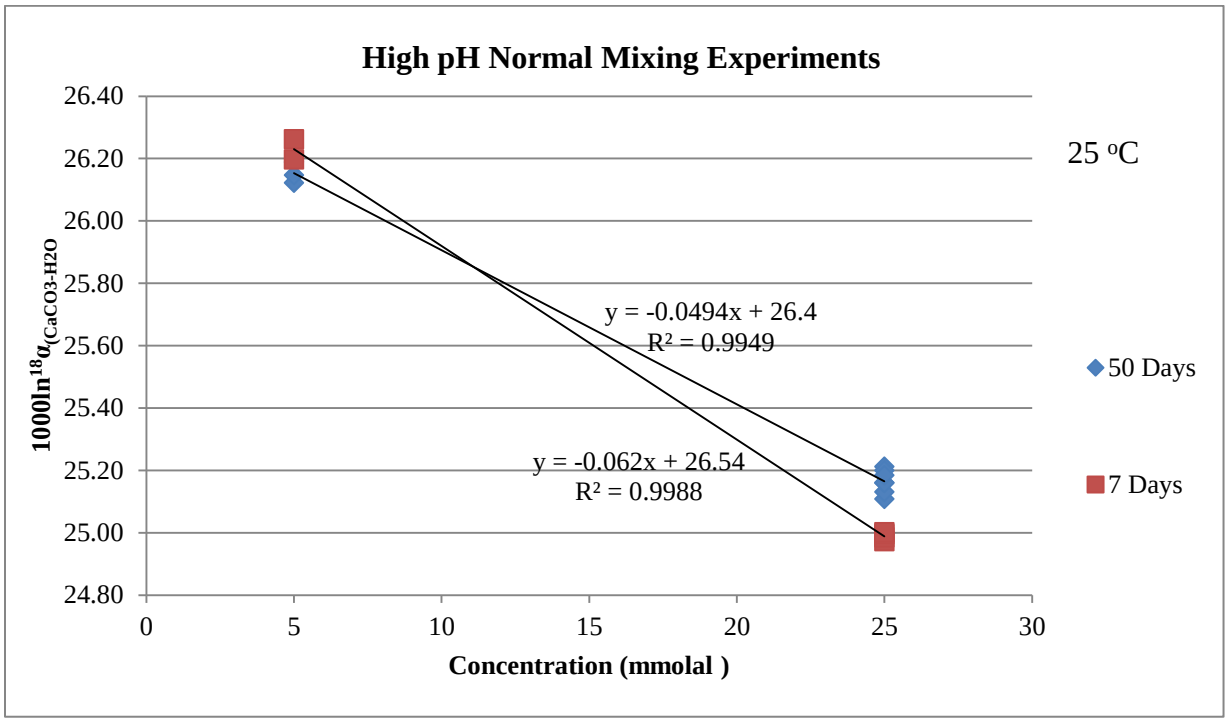

Figure 2.11: A comparison of the oxygen isotope fractionation factor between the 7 and 50 day samples.

References

Affek H. P. and Zaarur S. (2014) Kinetic isotope effect in CO_2 degassing: Insight from clumped and oxygen isotopes in laboratory precipitation experiments. *Geochim. Cosmochim. Acta* **143**, 319–330.

Aizawa K. and Miyachi S. (1984) Carbonic anhydrase located on cell surface increases the affinity for inorganic carbon in photosynthesis of Dunaliella tertiolecta. *FEBS Lett.* **173**, 41–44.

Badger M. R. (1994) The Role of Carbonic Anhydrase in Photosynthesis. *Annu. Rev. Plant Physiol. Plant Mol. Biol.* **45**, 369–392.

Beck W.C., Grossman E.L. and Morse J.W. (2005) Experimental studies of oxygen isotope fractionation factor in the carbonic acid system at 15 ºC, 25 ºC, and 40 ºC. *Geochimica et Cosmochimica Acta* **69**(14), 3493–3503.

Berg J., Tymoczko J. and Stryer L. (2002) Making a Fast Reaction Faster: Carbonic Anhydrases. In *Biochemistry*.

Bertucci A., Tambutté S., Supuran C. T., Allemand D. and Zoccola D. (2011) A New Coral Carbonic Anhydrase in Stylophora pistillata. *Mar. Biotechnol.* **13**, 992–1002.

Bradfield, J. R. G. (1947) Plant Carbonic Anhydrase. *Nature* **159**, 467–468.

Broecker W. S. (1986). Oxygen isotope constraints on surface ocean temperatures. *Quaternary Research* **26**(1), 121–134.

Chacko T. and Deines P. (2008). Theoretical calculation of oxygen isotope fractionation factors in carbonate systems. *Geochimica et Cosmochimica Acta* **72**(15), 3642– 3660.

Chang R. and Goldsby K. A. (2013) Chemistry. *McGraw-Hill Education.* New York, NY. **11**, pp. 180.

Coplen T. B. (2007) Calibration of the Calcite-Water Oxygen-Isotope Geothermometer at Devils Hole, Nevada, a natural laboratory. *Geochimica et Cosmochimica Acta* **71**(16), 3948-3957.

Dawson T. E., Mambelli S., Plamboeck A. H., Templer P. H. and Tu K. P. (2002) Stable isotopes in plant ecology. *Annu. Rev. Ecol. Syst.* **33**, 507–559.

Deines P. (2005). Comment on An explanation of the effect of seawater carbonate concentration on foraminiferal oxygen isotopes, by RE Zeebe (1999). *Geochimica et cosmochimica acta* **69**(3), 787-790.

De Villiers S., Nelson B.K. and Chivas A.R. (1995) Biological controls on coral Sr/Ca and δ18O reconstructions of sea surface temperatures. *Science* **269**, 1247–1249.

Donaldson T. and Quinn J. A. (1974) Kinetic constants determined from membrane transport measurements: carbonic anhydrase activity at high concentrations. *Proc. Natl. Acad. Sci. U. S. A.* **71**, 4995–4999.

Dietzel M., Tang J., Leis A. and Köhler S. J. (2009) Oxygen isotopic fractionation factor during inorganic calcite precipitation — Effects of temperature, precipitation rate and pH. *Chem. Geol.* **268**, 107–115.

Epstein S., Buchsbaum R., Lowenstam H., and Urey H. (1953). Revised CarbonateWater Isotopic Temperature Scale. Geological Society of America Bulletin, 11, 1315–1326.

Furla P., Allemand D. and Orsenigo M. N. (2000) Involvement of H(+)-ATPase and carbonic anhydrase in inorganic carbon uptake for endosymbiont photosynthesis. *Am. J. Physiol. Regul. Integr. Comp. Physiol.* **278**, R870–R881.

Gabitov R. I., Watson E. B. and Sadekov A. (2012) Oxygen isotope fractionation factor between calcite and fluid as a function of growth rate and temperature: An in situ study. *Chem. Geol.* **306-307**, 92–102.

Guo W., Mosenfelder J. L., Goddard W. A. and Eiler J. M. (2009) Isotopic fractionation factors associated with phosphoric acid digestion of carbonate minerals : Insights from first-principles theoretical modeling and clumped isotope measurements. *Geochim. Cosmochim. Acta* **73**, 7203–7225.

Hatch M. D. and Burnell J. N. (1990) Carbonic anhydrase activity in leaves and its role in the first step of c(4) photosynthesis. *Plant Physiol.* **93**, 825–8.

Hendy C. (1971) The isotopic geochemistry of speleothems - I. The calculation of the effects of different modes of formaion on the isotopic composition of speleothems and their applicability as paleoclimatic indicators. *Geochim. Cosmochim. Acta* **35**, 801–824.

Hewett-Emmett D. and Tashian R. E. (1996) Functional Diversity, Conservation, and Convergence in the Evolution of the α-, β-, and γ-Carbonic Anhydrase Gene Families. *Mol. Phylogenet. Evol.* **5**, 50–77.

Jackson D. J., Macis L., Reitner J., Degnan B. M. and Wörheide G. (2007) Sponge paleogenomics reveals an ancient role for carbonic anhydrase in skeletogenesis. *Science (80-.).* **316**, 1893–1895.

Jimenez-Lopez C., Caballero E., Huertas F. J. and Romanek, C. S. (2001) Chemical, mineralogical and isotope behavior, and phase transformation during the precipitation of calcium carbonate minerals from intermediate ionic solution at 25 ° C. *Geochimica et Cosmochimica Acta* **65(19)**, 3219–3231.

Kernohan J.C. (1964) The pH - activity curve of bovine carbonic anhydrase and its relationship to the inhibition of the enzyme by anions. *Biochim. Biophys. Acta* **96**, 304-317.

Kieffer S.W. (1982) Thermodynamic and lattice vibrations of minerals: 4. Application tom phase equilibria, isotope fractionation, and high pressure thermodynamics properties. *Rev. Geophys. Space Phys.* **20**, 827-849.

Kim S. and O'Neil J. (1997) Equilibrium and nonequilibrium oxygen isotope effects in synthetic carbonates. *Geochimica et Cosmochimica Acta* **61**(16), 3461–3475.

Kim S., Hillaire-Marcel C. and Mucci A. (2006) Mechanisms of equilibrium and kinetic oxygen isotope effects in synthetic aragonite at 25ºC. *Geochimica et Cosmochimica Acta* **70**, 5790-5801.

Kim S.-T., O'Neil J. R., Hillaire-Marcel C. and Mucci A. (2007) Oxygen isotope fractionation factor between synthetic aragonite and water: Influence of temperature and Mg2+ concentration. *Geochim. Cosmochim. Acta* **71**, 4704–4715.

Kluge T. and John C. M. (2015) Technical Note: A simple method for vaterite precipitation for isotopic studies: Implications for bulk and clumped isotope analysis. *Biogeosciences* **12**, 3289–3299.

ter Kuile B., Erez J. and Padan E. (1989) Competition for inorganic carbon between photosynthesis and calcification in the symbiont-bearing foraminifer Amphistegina lobifera. *Mar. Biol.* **103**, 253–259.

Lamb J. E. (1977) Plant carbonic anhydrase. *Life Sci.* **20**, 393–406.

Lide D. R. (2005) CRC Handbook of Chemistry and Physics. *Boca Raton (FL): CRC Press.* **86**, 90.

Liljas A. and Laurberg M. (2000) A Wheel Invented Three Times: The Molecular Structures of the Three Carbonic Anhydrases. *EMBO* **1**, 16–17.

Lindskog S. and Coleman J. E. (1973) The catalytic mechanism of carbonic anhydrase. *Proc. Natl. Acad. Sci. U. S. A.* **70**, 2505–2508.

McCrea J. M. (1950) On the isotopic chemistry of carbonates and a paleotemperature scale. *Journal of Chemical Physics* **18**(6), 849–857.

Mickler P. J., Banner J. L., Stern L., Asmerom Y., Edwards R. L. and Ito E. (2004) Stable isotope variations in modern tropical speleothems: Evaluating equilibrium vs. kinetic isotope effects. *Geochim. Cosmochim. Acta* **68**, 4381–4393.

Mills G.A. and Urey H.C. (1940) The kinetics of isotopic exchange between carbon dioxide, bicarbonate ion, carbonate ion, and water. *J. Am. Chem. Soc.* **62**, 1019-1026.

Mook W. G. (2000) Environmental isotopes in the hydrological cycle Volume I.pdf. *Tech. Doc. Hydrol.* **1**, 1–291.

Moroney J. V., Bartlett S. G. and Samuelsson G. (2001) Carbonic anhydrases in plants and algae: Invited review. *Plant, Cell Environ.* **24**, 141–153.

Moya A., Tambutté S., Bertucci A., Tambutté E., Lotto S., Vullo D., Supuran C. T., Allemand D. and Zoccola D. (2008) Carbonic anhydrase in the scleractinian coral Stylophora pistillata: characterization, localization, and role in biomineralization. *J. Biol. Chem.* **283**, 25475–25484.

O'Leary M. H. (1981) Carbon isotope fractionation factor in plants. *Phytochemistry* **20**, 553–567.

O'Leary M. H. (1988) Carbon isotopes in photosynthesis. *Bioscience* **38**, 328–336.

Palmer A. N. (2007) Cave Geology. *Cave Books.* Dayton, OH. pp. 275.

Raven J. A. (1995) Photosynthetic and non-photosynthetic roles of carbonic anhydrase in algae and cyanobacteria. *Phycologia* **34**, 93–101.

Reed M.L. and Graham D. (1981). Carbonic anhydrase in plants: distribution, properties and possible physiological roles. In: Reinhold L, Harborne JB, Swain T, editors. *Progress in Phytochemistry*. Oxford, UK: Pergamon Press. **7**, pp. 47–94.

Romanek C. S., Grossman E. L. and Morse J. W. (1992) Carbon isotopic fractionation factor in syntetic aragonite and calcite: effects of temperature and precipitation rate. *Geochim. Cosmochim. Acta* **56**, 419–430.

Roughton F. J. and Booth V. H. (1946) The effect of substrate concentration, pH and other factors upon the activity of carbonic anhydrase. *Biochem. J.* **40**, 319–30.

Schauble E. a., Ghosh, P., and Eiler, J. M. (2006). Preferential formation of 13C–18O bonds in carbonate minerals, estimated using first-principles lattice dynamics. *Geochimica et Cosmochimica Acta* **70**(10), 2510–2529.

Soto A. R., Zheng H., Shoemaker D., Rodriguez J., Read B. A. and Wahlund T. M. (2006) Identification and preliminary characterization of two cDNAs encoding unique carbonic anhydrases from the marine alga Emiliania huxleyi. *Appl. Environ. Microbiol.* **72**, 5500–5511.

Spero H. J., Bijma J., Lea D. W. and Bemis, B. E. (1997). Effect of seawater carbonate concentration on foraminiferal carbon and oxygen isotopes. *Nature* **390**, 497–500.

Staddon P. L. (2004) Carbon isotopes in functional soil ecology. *Trends Ecol. Evol.* **19**, 148–154.

Sültemeyer D. (1998) Carbonic anhydrase in eukaryotic algae: characterization, regulation, and possible function during photosynthesis. *Can. J. Bot.* **76**, 962–972.

Takita Y., Eto M., Sugihara H. and Nagaoka K. (2007) Promotion mechanism of co-existing NaCl in the synthesis of CaCO3. *Mater. Lett.* **61**, 3083–3085.

Tambutté S., Tambutté E., Zoccola D., Caminiti N., Lotto S., Moya A., Allemand D. and Adkins J. (2007) Characterization and role of carbonic anhydrase in the calcification process of the azooxanthellate coral Tubastrea aurea. *Mar. Biol.* **151**, 71–83.

Tarutani T., Clayton R. N. and Mayeda, T. K. (1969). The effect of polymorphism and magnesium substitution on oxygen isotope fractionation factor between calcium carbonate and water. *Geochimica et Cosmochimica Acta* **33**, 987–996.

Tripp B. C., Smith K. and Ferry J. G. (2001) Carbonic Anhydrase: New Insights for an Ancient Enzyme. *J. Biol. Chem.* **276**, 48615–48618.

Turner J. V. (1982). Kinetic fractionation factor of carbon-13 during calcium carbonate precipitation. *Geochimica et Cosmochimica Acta* **46**(7), 1183–1191.

Uchikawa J. and Zeebe R. E. (2012) The effect of carbonic anhydrase on the kinetics and equilibrium of the oxygen isotope exchange in the CO_2-H_2O system: Implications for $\delta^{18}O$ vital effects in biogenic carbonates. *Geochim. Cosmochim. Acta* **95**, 15–34.

Urey, H. C. (1947). The Thermodynamic Properties of Isotopic Substances. Journal of the Chemical Society, 562-581.

Usdowski, E. and Hoefs, J. (1990). Kinetic 13C/12C and 18O/16O effects upon dissolution and outgassing of CO2 in the system CO2-H2O. Chemical Geology (Isotope Geosciences Edition), 80, 109–118.

Voigt O., Adamski M., Sluzek K. and Adamska M. (2014) Calcareous sponge genomes reveal complex evolution of α -carbonic anhydrases and two key biomineralization enzymes Calcareous sponge genomes reveal complex evolution of α -carbonic anhydrases and two key biomineralization enzymes.

Watkins J. M., Nielsen L. C., Ryerson F. J. and DePaolo D. J. (2013) The influence of kinetics on the oxygen isotope composition of calcium carbonate. *Earth Planet. Sci. Lett.* **375**, 349–360.

Wickman F. E. (1952) Variations in the relative abundance of the carbon isotopes in plants. *Geochim. Cosmochim. Acta* **2**, 243–254.

Zeebe R. E. (1999) An explanation of the effect of seawater carbonate concentration on foraminiferal oxygen isotopes. *Geochimica et Cosmochimica Acta* **63**, 2001-2007.

Zeebe R. (2007). An explanation of the effect of seawater carbonate concentration on foraminiferal oxygen isotopes. *Geochimica et Cosmochimica Acta* **63**(13), 2001– 2007.

Chapter 3:

Conclusions, Contributions, and Future Research

Chapter 3

"The man who moves a mountain begins by carrying away small stones".

– Confucius

3.1 Summary of Findings

The results of these experiments will help to improve the effectiveness of carbonates as a paleoclimate indicator. The measurement of the $\delta^{18}O$ and $\delta^{13}C$ values within the synthetic calcite crystals stand to further assist researchers by providing a tool to correlate their measured isotopic fractionation factors and provide a deeper understanding of the paleoclimate of their studied area. This study also built upon the current knowledge and observations regarding how environmental factors, such as temperature, influence the $\delta^{18}O$ and $\delta^{13}C$ values in natural calcite raft samples. Calcite was synthesized through the reaction of sodium bicarbonate ($NaHCO_3$) and calcium chloride dihydrate ($CaCl_2 \cdot 2H_2O_{(aq)}$) at 5, 15 and 25 mmolal concentrations using three different synthesis techniques to control precipitation rate. Carbonate samples precipitated using the Normal Mixing technique were taken from the surface, sides and bottom of the bottles in which the carbonates precipitated. It was found that there was no difference in the $1000\ln{}^{18}\alpha_{(CaCO_3\text{-}H_2O)}$ for oxygen and $1000\ln{}^{13}\alpha_{(CaCO_3\text{-}DIC)}$ for oxygen regardless of location within the bottle. This trend is believed to have been caused by the production of $CO_{2(aq)}$ as a by-product of the reaction between $NaHCO_3$ and $CaCl_2$ (degassing from Type II CPM). This would have caused an enrichment in the DIC since lighter isotopologues of $CO_{2(aq)}$ would preferentially leave the water system since these isotopes would have been preferentially incorporated into the carbon dioxide. This effect increased with concentration and it is for this reason that the carbonate samples collected from 25 mmolal concentrations were heavier than the 5 or 15 mmolal samples in both oxygen and carbon. Unlike the $CO_{2(g)}$ degassing trend observed in

Affek and Zaarur (2014), which strictly occurred at the air-water boundary (Type I CPM) and enriched the surface carbonates more than those which formed at the bottom of the solution, Type II CPM enriched all of the carbonates within the bottle equally. Additionally, samples were stored in a growth chamber kept at $25 \pm 0.1\,^{o}C$ for 1, 3, 5 and 7 weeks and were found to remain consistent over time. This suggests that the samples precipitated in less than a week and did not change its isotopic fractionation factor values afterwards.

Samples were also precipitated from NaCl containing solutions in an open system. The morphology of these samples were then compared to the samples which had also been precipitated from low ionic strength solutions under an open system. It was found that those which precipitated from NaCl containing solutions always yielded 100% calcite, like the samples precipitated under a closed system. However, the open, low ionic strength solutions were composed of ~25 % vaterite. It is believed that the presence of the meta-stable vaterite signifies that the precipitation rate of these samples was very fast and therefore precipitated as the most unstable form of calcium carbonate, since there was not enough time for the crystal to completely convert to the more stable polymorph, calcite. However, it is believed that the presence of NaCl in the precipitating solutions increased the solubility of the carbonate and slowed the precipitation rate enough to allow the more stable calcite to form (Takia et al., 2007). This conflicts with the findings of Kluge and John (2014), who precipitated vaterite in the presence of NaCl. However, that study utilized active $CO_{2(g)}$ degassing to precipitate carbonate, which would have precipitated the carbonate quickly, regardless of the presence of NaCl and negated its effect on the morphology.

Carbonates precipitated under these conditions also showed a positive linear trend in the $1000\ln^{18}\alpha_{(CaCO_3\text{-}H_2O)}$ and $1000\ln^{13}\alpha_{(CaCO_3\text{-}DIC)}$ values with increasing reactant concentration, and

thereby kinetic effects due to the faster precipitation rate which caused the precipitating carbonates to incorporate CO_3^{2-} which were not given enough time for re-equilibration after deprotonation and thereby retain the isotopic signature of the HCO_3^-. The system was also influenced $CO_{2(aq)}$ production caused by Type II CPM. Carbonate samples which precipitated at 5 mmolal concentration had permil oxygen isotope fractionation factor which were close to the equilibrium value of 28.3 ‰ between calcite and water proposed by Kim and O'Neil (1997) and the higher 25 and 50 mmolal experiments (as well as the open low ionic strength carbonates) seemed to plateau at the value 29.8 ‰ suggested by Coplen (2007). In all experiments conducted by this study, the initial carbonates precipitated in isotopic equilibrium with the parent water and deviated with an increasing amount of kinetic effects, following a Rayleigh distillation curve, causing the higher concentrated samples to deviate further from oxygen and carbon isotopic equilibrium. This may imply that the measured isotopic fractionation factor of a carbonate is actually an average of an entire spectrum of isotopic compositions which varied as the carbonate continued to grow, with this range increasing with concentration. Thus, perhaps 29.8 ‰ does not represent oxygen isotope equilibrium between calcite and water, but rather the average between 28.3 ‰ and the oxygen isotope fractionation factor between HCO_3^- and water of 31 ‰ as suggested by Beck et al. (2005).

The enzyme, carbonic anhydrase (CA) was also used in this study in an attempt to hasten the oxygen isotope equilibration time between DIC and water. Since the isotopic composition of carbonates are due to the interaction of three different processes: CO_2 degassing/production, CaCO3 precipitation rate, and isotopic equilibration between two phases such as DIC and water. Different CA concentrations were utilized using concentrations proposed by both Uchikawa and Zeebe (2012) and Watkins et al. (2013) and it was found that none of the carbonate samples were

able to attain oxygen isotope equilibrium with respect to parent solutions – despite a concentration of CA being used which would have caused the DIC and water to equilibrate almost immediately. This suggests that CA may not be able to significantly influence the isotopic composition of fast growing carbonates such as speleothems. Thus, if the naturally produced CA enzyme made it into the carbonate system, it may not be necessarily reflected in the isotopic composition of the carbonate and shows that this fast-acting catalyst has some limitations.

High pH experiments were conducted by using Na_2CO_3 and $CaCl_2$ at 5, 15, and 25 mmolal concentrations. Unlike the mid-pH experiments, the high pH experiments illustrated a negative linear trend the $1000\ln^{13}\alpha_{(CaCO_3\text{-}DIC)}$ values increased with concentration, but the $1000\ln^{18}\alpha_{(CaCO_3\text{-}H_2O)}$ decreased. Since $CO_{2(aq)}$ not forming as a by-product of Na_2CO_3 and $CaCl_2$ in this system, no trend was observed in the carbon isotope fractionation observed within the precipitating carbonate. In contrast, the oxygen isotope fractionation factor between carbonate and water declined with increasing concentration of the reactants since the CO_3^- ions were significantly dominant at the solution's pH (~11.07). Thus the faster precipitating carbonates, which formed under higher concentrations, would have incorporated a greater amount of the CO_3^- ions and had an oxygen isotope fractionation factor which was closer to the CO_3^{2-} oxygen isotope fractionation line compared to those which precipitated slower. It was also found that the trend line of the high pH solution intersects with those of the mid-pH experiments around 28.3 ‰, further suggesting that this value represents isotopic equilibrium between calcite and water.

Finally, two different DIC-water equilibration times, 7 and 50 days, were utilized before the addition of $CaCl_2$ based on the findings of Beck et al. (2005) and Kim et al. (2006). The results found that the $1000\ln^{18}\alpha_{(CaCO_3\text{-}H_2O)}$ and $1000\ln^{13}\alpha_{(CaCO_3\text{-}DIC)}$ values between both sets of samples were similar and suggests that equilibrium between DIC and water must have been

attained at 7 days before the onset of carbonate growth. However, this finding conflicts with the equilibration time of Beck et al. (2005) and may be related to the solutions of that study having ~100 % of DIC reservoir being composed of CO_3^- ions instead of the lower amounts observed in Kim et al. (2006) or the experiments of this manuscript.

The findings of this study illustrate that while carbonates synthesized in the laboratory precipitate faster than natural samples, it does not imply that they cannot attain isotopic equilibrium. This is because kinetic effects are not strictly determined by precipitation rate alone, but also the equilibration time and amount of $CO_{2(g)}$ degassing. If either the level of $CO_{2(g)}$ degassing or precipitation rate exceed the equilibration time, then the carbonate will precipitate in isotopic disequilibrium.

3.2 The Candidate's Contributions to this Research

The candidate had conducted all of the necessary background research, compiled the information, and provided a literature review. The candidate also conducted all of the experiments outlined in this manuscript, analyzed all of the precipitated carbonate samples using IRMS and solution samples through CF-IRMS to obtain and interpret carbon and oxygen isotope data. The candidate then wrote this manuscript and created all of the figures and tables by incorporating scientific and editorial feedback provided by the candidate's supervisor, Dr. Sang-Tae Kim and selected reviewers.

3.3 Future Research

Future research could synthesize carbonates using the same synthesis techniques described above and compare the results with those of this paper. These experiments should also utilize varying concentrations of CA to determine whether its effect is enhanced at lower temperatures. Sanyal and Maren (1981) found that the effect of CA in catalyzing the CO_2 hydration is invariant between 0 and 37 ^oC. Therefore, it is possible that CA might allow the

equilibration rate to outpace precipitation rate and $CO_{2(g)}$ degassing with declining temperature. It would also be worth precipitating carbonates at different concentration rates using the constant addition method in the presence of CA to determine the threshold in which this enzyme influences the isotopic composition of carbonates. Similarly, carbonates could also be precipitated using passive $CO_{2(g)}$ degassing under the open system under varying concentrations of NaCl to determine the point in which the precipitation of vaterite is hindered. This experiment could also vary the surface area of the air-water boundary to influence the rate of Type II CPM.

Using the constant addition method, carbonates may also be conducted under a closed system through the reaction of $NaHCO_3^-$ and $CaCl_2$ while examining the isotope fractionation factor value at different growth intervals as per the techniques used in Gabitov et al. (2012). This can provide direct evidence of whether the initial portion of the carbonate to precipitate was close to the equilibrium value proposed by Coplen (2007). If the conclusion of this manuscript is correct, then the fractionation factor of the sample should decrease from the center towards the edges of the crystal and a higher concentration should provide a spectrum which averages around the value proposed by Coplen (2007).

It would also be worth conducting clumped isotope analysis on the samples precipitated in these experiments. Clumped isotope thermometry utilizes the fact that the relative abundance of $^{13}C^{18}O^{16}O$ in $CO_{2(g)}$ produced through carbonate acid digestion varies based on their formation temperature, with a greater amount of "clumping" occurring at lower temperatures. Preliminary tests on the samples have shown that there is no difference in the Δ_{47} of the samples, regardless of concentration, pH, or whether CA was present. This suggests that the clumped isotope

paleothermometer is unaffected by the aforementioned conditions under the studied system. However, more analysis is required before this finding can be verified.

The results of this study can be further expanded upon by testing the oxygen and carbon isotope effects in biogenic carbonates, such as foraminifera, at the same pH to test if the same carbon and oxygen enrichment trend would be observed. Growth rate can be controlled by varying factors such as light availability or salinity level. Since these experiments would introduce vital effects as an additional source of kinetic fractionation, only one species should be studied at a time. This would eliminate the need to consider vital effects as an additional factor since this process shall influence all samples equally. Future experiments can then repeat these experimental procedures using different species and comparing the results.

References

Affek H. P. and Zaarur S. (2014) Kinetic isotope effect in CO_2 degassing: Insight from clumped and oxygen isotopes in laboratory precipitation experiments. *Geochim. Cosmochim. Acta* **143**, 319–330.

Beck W.C., Grossman E.L. and Morse J.W. (2005) Experimental studies of oxygen isotope fractionation factor in the carbonic acid system at 15 ºC, 25 ºC, and 40 ºC. *Geochimica et Cosmochimica Acta* **69**(14), 3493–3503.

Coplen T. B. (2007) Calibration of the Calcite-Water Oxygen-Isotope Geothermometer at Devils Hole, Nevada, a natural laboratory. *Geochimica et Cosmochimica Acta* **71**(16), 3948-3957.

Gabitov R. I., Watson E. B. and Sadekov A. (2012) Oxygen isotope fractionation factor between calcite and fluid as a function of growth rate and temperature: An in situ study. *Chem. Geol.* **306-307**, 92–102.

Kim S. and O'Neil J. (1997) Equilibrium and nonequilibrium oxygen isotope effects in synthetic carbonates. *Geochimica et Cosmochimica Acta* **61**(16), 3461–3475.

Kim S., Hillaire-Marcel C. and Mucci A. (2006) Mechanisms of equilibrium and kinetic oxygen isotope effects in synthetic aragonite at 25ºC. *Geochimica et Cosmochimica Acta* **70**, 5790-5801.

Kluge T. and John C. M. (2015) Technical Note: A simple method for vaterite precipitation for isotopic studies: Implications for bulk and clumped isotope analysis. *Biogeosciences* **12**, 3289–3299.

Sanyal G. and Maren T. H. (1981) Thermodynamics of Carbonic Anhydrase Catalysis. *J. Biol. Chem.* **256**, 608–612.

Uchikawa J. and Zeebe R. E. (2012) The effect of carbonic anhydrase on the kinetics and equilibrium of the oxygen isotope exchange in the CO_2-H_2O system: Implications for $\delta^{18}O$ vital effects in biogenic carbonates. *Geochim. Cosmochim. Acta* **95**, 15–34.

Watkins J. M., Nielsen L. C., Ryerson F. J. and DePaolo D. J. (2013) The influence of kinetics on the oxygen isotope composition of calcium carbonate. *Earth Planet. Sci. Lett.* **375**, 349–360.